EUROPEAN COMMISSION

Community Research

SEVENTH FRAMEWORK PROGRAMME

CARBOWASTE

Treatment and Disposal of Irradiated Graphite and Other Carbonaceous Waste

Grant Agreement Number: FP7-211333

Deliverable T-6.1.3 / T-3.2.2-b

REPORT ON MOBILITY AND LEACHING OF CHLORINE IN CL-IMPLANTED GRAPHITE

Author(s): C.E. Vaudey, N. Toulhoat, N. Moncoffre, N. Bérerd

Institut de Physique Nucléaire de Lyon – CNRS/IN2P3 – Université Lyon 1

Date of first issue of this report : April 2011

Start date of the project : **01/04/2008** Duration : **48 Months**

Project co-funded by the European Commission under the Seventh Framework Programme (2007 to 2011) of the European Atomic Energy Community (EURATOM) for nuclear research and training activities

Dissemination Level

PU	Public	**X**
RE	Restricted to the partners of the CARBOWASTE project	
CO	Confidential, only for specific distribution list defined on this document	

Distribution list

Person and organisation name and/or group	Comments
CARBOWASTE Project Participants	
European Commission	

CARBOWASTE		
Work package: 6 **Task: :** 6.1	**CARBOWASTE document no:** CARBOWASTE-1104-T-6.1.3	**Document type: D**
Issued by: IPNL **Internal no.:** CW1104-Deliverable-T-6-1-3-IPNL		**Document status:** Final

Document title

REPORT ON MOBILITY AND LEACHING OF CHLORINE IN CL- IMPLANTED GRAPHITE

Executive summary

The effects of temperature on chlorine's behaviour were studied using ^{37}Cl ion implantation into graphite samples that allows simulating ^{36}Cl atoms displaced from their original structural site through recoil in reactor condition. The results show clearly that the main migration mechanism proceeds through a quasi athermal release of ^{36}Cl through the graphite's open pores. Around 20 to 30 % chlorine is released into the cooling gas since the very beginning of the reactor operation. Another part of chorine is released all over the reactor life. Two release steps have been identified. The kinetics of the first one is very fast and the activation energy is lower than 0.5 eV. The second one is much slower and long duration thermal annealing is still underway in order to determine the release kinetics of this second step. The two fractions correspond to two distinct chemical forms of chlorine having different thermal stabilities or to two distinct locations.

SIMS analysis and imaging show that the chlorine distribution is very heterogeneous with the occurrences of some small "hot spots" (dimension lower that 5 µm) where chlorine is combined to neither metals nor oxygen. This distribution reflects the heterogeneous composition of nuclear graphite at the micron scale. No gaseous Cl_2 has been identified.
TDS was used to determine chlorine's chemical form released in the gas. The results confirm the release of chlorine at low temperature and show that chlorine is released as HCl.

The XPS and XANES techniques were used to determine chlorine's speciation in graphite. These experiments were conducted on virgin and annealed samples. They show that a small fraction of the early released chlorine corresponds to oxychloride compounds covering the pore's walls and released through the open pores. This fraction results mainly from the purification stage during graphite manufacturing and is thermally very labile. The main speciation of chlorine in nuclear graphite is however organic (resulting mainly from the impurities of coke and pitch). This form has a better thermal stability and is not easily released except if located near open pores.

Concerning the behavior of chlorine during leaching, our results show that the inorganic form should be very labile to leaching mainly because of its location on the pore walls. Our results also show that irradiation induces a strong disorder of the graphite matrix and that, during reactor operation, the temperature effect tends to reorder the graphite matrix. The reordering level depends on the temperature but, generally, the graphite does not get its original structure back because this would require very high temperatures (close to graphitization temperatures, i.e. higher than 2000°C). Therefore, depending on the neutron flux distribution in the reactor and the graphite temperature, there will be highly disordered zones with larger pores where chlorine will be more accessible to water and therefore to leaching. On the other hand, in the better structured and less porous zones, chlorine should be less accessible to leaching

The report also contributes to Deliverable T-3.2.2.

Revisions						
Rev.	Date	Short description	Author	Internal Review	Task Leader	WP Leader
0	April 2011	First issue	*Vaudey IPNL*	Toulhoat IPNL	Comte CEA	Grambow EMN
1	December 2011	Final	*Vaudey IPNL*	Toulhoat IPNL	Comte CEA	Grambow EMN

Table of contents

REPORT ON MOBILITY AND LEACHING OF CHLORINE IN CL- IMPLANTED GRAPHITE ---------- **2**

Introduction : nature of the nuclear graphite studied ---------- *2*
A. Thermal behaviour of implanted chlorine ---------- *5*
A.I Identification of the migration mechanism of chlorine in graphite : SIMS analyses ---------- 6
A.I.1) Study of the migration mechanism of chlorine ---------- 6
A.I.2) Effects of porosity and structural orientation of graphite ---------- 12
A.I.2).a) Nuclear graphite ---------- 12
A.I.2).b) "Model" graphite ---------- 15
A.I.2).c) Conclusion ---------- 17
A.II Following the evolution of the graphite structure by Raman microspectroscopy ---------- 17
A.III Following the evolution of the quantity of oxygen in nuclear graphite by resonating elastic retrodiffusion -- 21
A.IV Conclusion ---------- 23
B. Thermal behaviour of constitutive chlorine ---------- *24*
B.I Distribution of the constitutive chlorine ---------- 25
B.II Nature of gaseous species released during the thermal treatment ---------- 27
B.II.1) Desorption of oxygenated and hydrogen chloride species ---------- 27
B.II.2) Desorption of ethanol ---------- 29
B.II.3) Conclusion ---------- 30
B.III Evolutions of the density and mass of nuclear graphite during thermal treatment ---------- 31
B.IV Speciation of carbon and constitutive chlorine by photoelectron spectroscopy ---------- 32
B.IV.1) Characterisation of certain impurities in nuclear graphite ---------- 32
B.IV.1).a) Case of virgin nuclear graphite ---------- 32
B.IV.1).b) Effect of thermal treatment ---------- 33
B.IV.2) Speciation of carbon in nuclear graphite ---------- 34
B.IV.2).a) Case of virgin nuclear graphite ---------- 34
B.IV.2).b) Effect of thermal treatment ---------- 35
B.IV.3) Speciation of of constitutive chlorine in nuclear graphite ---------- 36
B.IV.3).a) Case of virgin nuclear graphite ---------- 36
B.IV.3).b) Effect of thermal treatment ---------- 38
B.IV.4) Conclusion ---------- 39
B.V Speciation of constitutive chlorine by X-ray absorption spectroscopy ---------- 39
B.V.1) Reference compounds ---------- 40
B.V.1).a) Reference compounds containing inorganic chlorine ---------- 40
B.V.1).b) Reference compounds containing organic chlorine ---------- 43
B.V.2) Nuclear graphite samples ---------- 46
B.V.2).a) Stability of chlorine under beam ---------- 46
B.V.2).b) Chlorine distribution ---------- 46
B.V.2).c) Case of virgin nuclear graphite ---------- 47
B.V.2).d) Effect of thermal treatment ---------- 49
B.V.3) Conclusion ---------- 50
B.VI Conclusion ---------- 50
C. Behavior of chlorine during lixiviation …… .50

LIST OF FIGURES ---------- **54**

LISTE OF TABLES ---------- **55**

Temperature effect on the behavior of chlorine in nuclear graphite

We present here the experimental study of the temperature effect on the behavior, distribution and speciation of chlorine in nuclear graphite. This chapter consists of two parts: the first concerns the study of the thermal behavior of chlorine implanted in the graphite. In fact, we have chosen to implant chlorine to create a known concentration gradient in the matrix in order to identify the migration mechanism of this element in graphite. The second part is dedicated to the characterization of the distribution and speciation of the naturally-occurring chlorine, henceforth known as "constitutive chlorine", in nuclear graphite. We analyzed the constitutive chlorine because, contrary to the implanted chlorine, the former is available in sufficient quantity in the volume of the matrix to make it possible to characterize the nature of the desorbed chlorine species in the graphite through the effect of temperature and thus identify its speciation.

Introduction : nature of the nuclear graphite studied

All of these studies were realized on four types of nuclear graphite samples: the sleeve and moderator from SLA2, and the reflector and moderator from G2. However, as illustrated in table 4-1, both the raw materials and purifying agents used during their fabrication are different in nature.

	Chemise de SLA2	Empilement de SLA2	Réflecteur de G2	Empilement de G2
Type de coke	Lima ou "à aiguilles"	Lima	Lockport	Spécial A
Diamètre des grains (en mm)	0,8 à 0,4	1,6 à 0,8	1,6 à 0,8	1,6 à 0,8
Nature de l'agent épurant	Non précisée	MgF_2 gazeux	NaF gazeux	NaF gazeux
Nbre d'imprégnations	2	1	1	1
Masse volumique (en g cm^{-3})	1,72	1,68	1,68	1,68

Table 4-1 : Raw materials, purifying agents and the characteristics of the nuclear graphite of the sleeve and moderator from SLA2, and reflector and moderator from G2

From the literature, all nuclear graphite contains impurities of the same nature (metals, oxygen, halogens, etc.), but at different concentrations [Chapter 2.II.3).a).ii]. In collaboration with L. Raimbault, we have confirmed this by analyzing the impurities contained in the graphite samples from the moderator from both G2 and SLA2 by instrumental neutron activation. The samples were irradiated for 8h, by a flux of epithermal and fast neutrons equal to $2.7 \times 10^{13} n.cm^{-2}.s^{-1}$ into the heart of the CEA Osiris reactor in Saclay. The radioactivity induced, principally according to the nuclear reactions of the type (n, γ), is measured by the means of a germanium crystal detector (Camberra) after a period of radioactive decay of seven days for the radio-isotopes ^{24}Na, ^{75}As, ^{82}Br, ^{99m}Tc (Mo), ^{117m}In (Cd), ^{140}La, ^{153}Sm, ^{187}W,

^{198}Au and ^{239}Np (U), and approximately one month for the other radio-isotopes. Table 4-2 gives the nature and mass concentration of the principal impurities contained in the nuclear graphite of the moderator from G2 and SLA2. These rates are calculated by comparing them with silicate rock standards of known composition (GS-N and GXR-4). The uncertainties indicated correspond to the statistical combination of sample and standard counting.

Nature de l'impureté	Concentration massique de l'impureté dans l'empilement de G2	Concentration massique de l'impureté dans l'empilement de SLA2
Na	20 ± 6 ppm	45 ± 9 ppm
Ca	< 130 ppm	< 150 ppm
Sc	0,60 ± 0,25 ppb	0,69 ± 0,29 ppb
Cr	< 0,1 ppm	< 0,2 ppm
Fe	3,7 ± 0,7 ppm	2,7 ± 0,7 ppm
Co	0,0204 ± 0,0021 ppm	0,0550 ± 0,0030 ppm
Ni	0,341 ± 0,022 ppm	3,060 ± 0,080 ppm
Zn	1,00 ± 0,08 ppm	1,11 ± 0,09 ppm
As	0,014 ± 0,004 ppm	0,029 ± 0,005 ppm
Se	< 6 ppb	3,7 ± 2,5 ppb
Br	0,021 ± 0,005 ppm	0,050 ± 0,006 ppm
Rb	0,026 ± 0,011 ppm	< 0,03 ppm
Sr	< 0,3 ppm	< 0,4 ppm
Zr	< 0,6 ppm	< 0,7 ppm
Mo	0,309 ± 0,008 ppm	0,157 ± 0,007 ppm
Ag	18,1 ± 1,1 ppb	125,1 ± 2,8 ppb
Cd	< 0,06 ppm	< 0,09 ppm
Sn	0,083 ± 0,025 ppm	0,15 ± 0,04 ppm
Sb	1,7 ± 0,4 ppb	5,4 ± 0,7 ppb
Cs	1,65 ± 0,26 ppb	3,10 ± 0,40 ppb
Ba	< 0,3 ppm	< 0,4 ppm
La	0,014 ± 0,006 ppm	0,066 ± 0,011 ppm
Ce	< 0,06 ppm	0,11 ± 0,03 ppm
Nd	< 0,11 ppm	< 0,20 ppm
Sm	0,38 ± 0,13 ppb	2,90 ± 0,50 ppb
Eu	1,4 ± 0,5 ppb	1,4 ± 0,7 ppb
Gd	< 3 ppb	< 4 ppb
Tb	< 0,2 ppb	0,29 ± 0,10 ppb
Yb	< 3 ppb	< 4 ppb
Hf	< 3 ppb	< 3 ppb

Ta	0,74 ± 0,16 ppb	1,31 ± 0,19 ppb
W	0,029 ± 0,010 ppm	< 0,04 ppm
Au	0,116 ± 0,016 ppb	0,650 ± 0,030 ppb
Th	< 0,7 ppb	0,50 ± 0,25 ppb
U	< 2 ppb	4,4 ± 0,7 ppb

Table 4-2 : Nature and concentration of the principal impurities of the graphite from G2 and SLA2 moderator determined by neutron activation

The results in the table show that some metals (Fe, Ni and Zn) and sodium are the most abundant impurities, present at the rates of a few ppm to some tens of ppm, respectively. However, their concentrations can be significantly different for the two types of nuclear graphite. For example, the rate in Ni is 0.34 ppm (by mass) in the graphite of the moderator from G2, whereas it reaches 3 ppm (by mass) in the SLA2 graphite moderator.

A. Thermal behavior of implanted chlorine

The data obtained in this study concern on the one hand, the identification and the characterization of the migration mechanism of chlorine in graphite, and on the other hand, the evolution of the graphite structure and its concentration in oxygen during the different steps of the experimental protocol. To realize this study, we have used the following protocol. (Figure 4-1) First, the samples were cut, polished to the nearest micrometer using diamond paste diluted in ultra-pure ethanol, and pre-annealed at 1000°C during 8 h in order to remove some of the polishing defects. Then, we chose to implant ^{37}Cl in the graphite at a fluence of $5x10^{13}$ per cm^{-2} and an energy of 200 or 250 keV, in order to simulate the ^{36}Cl which is activated then displaced from its structural site during the time spent in the reactor in the nuclear graphite. After that, the samples underwent heat treatment between 200 and 1100 °C during 2 or 4 hours to reveal the thermal behavior of chlorine. Finally, we determined the chlorine profiles using an ionic microprobe, characterized the graphite structure by Raman microspectroscopy and quantified the quantity of oxygen in the matrix by nuclear backscattering spectrometry.

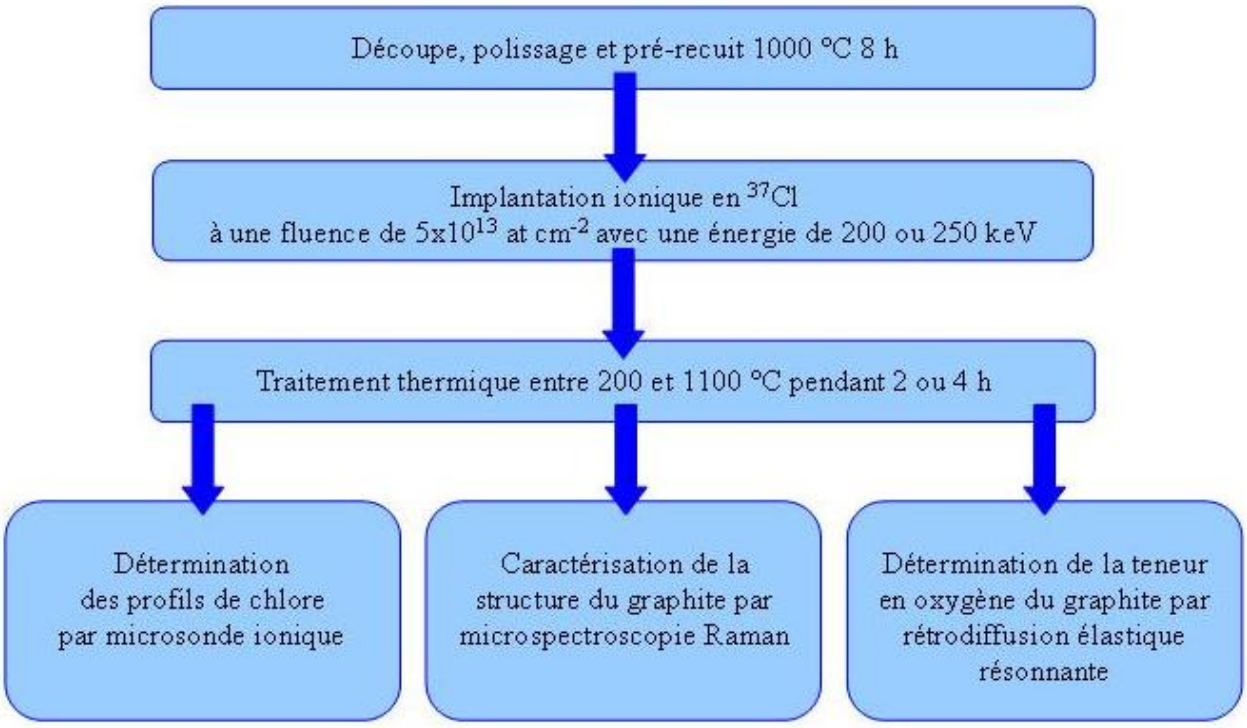

Figure 4-1 : Schematic of the experimental protocol used for studying the thermal behavior of chlorine implanted in graphite

A.I Identification of the migration mechanism of chlorine in graphite: SIMS analysis

We wanted to determine the migration mechanism of chlorine in nuclear graphite and study the effects of the texture and structural orientation of the matrix on this migration phenomenon.

A.I.1) Study of the migration mechanism of chlorine

This study was led on nuclear graphite samples from the sleeve and moderator from SLA2, and the reflector from G2. The ^{37}Cl profiles obtained by SIMS profilometry for both implanted samples and those annealed are presented in figure 4-2. Each profile corresponds to the average of at least two profiles, which allowed us to confirm the reproducibility of our analyses.

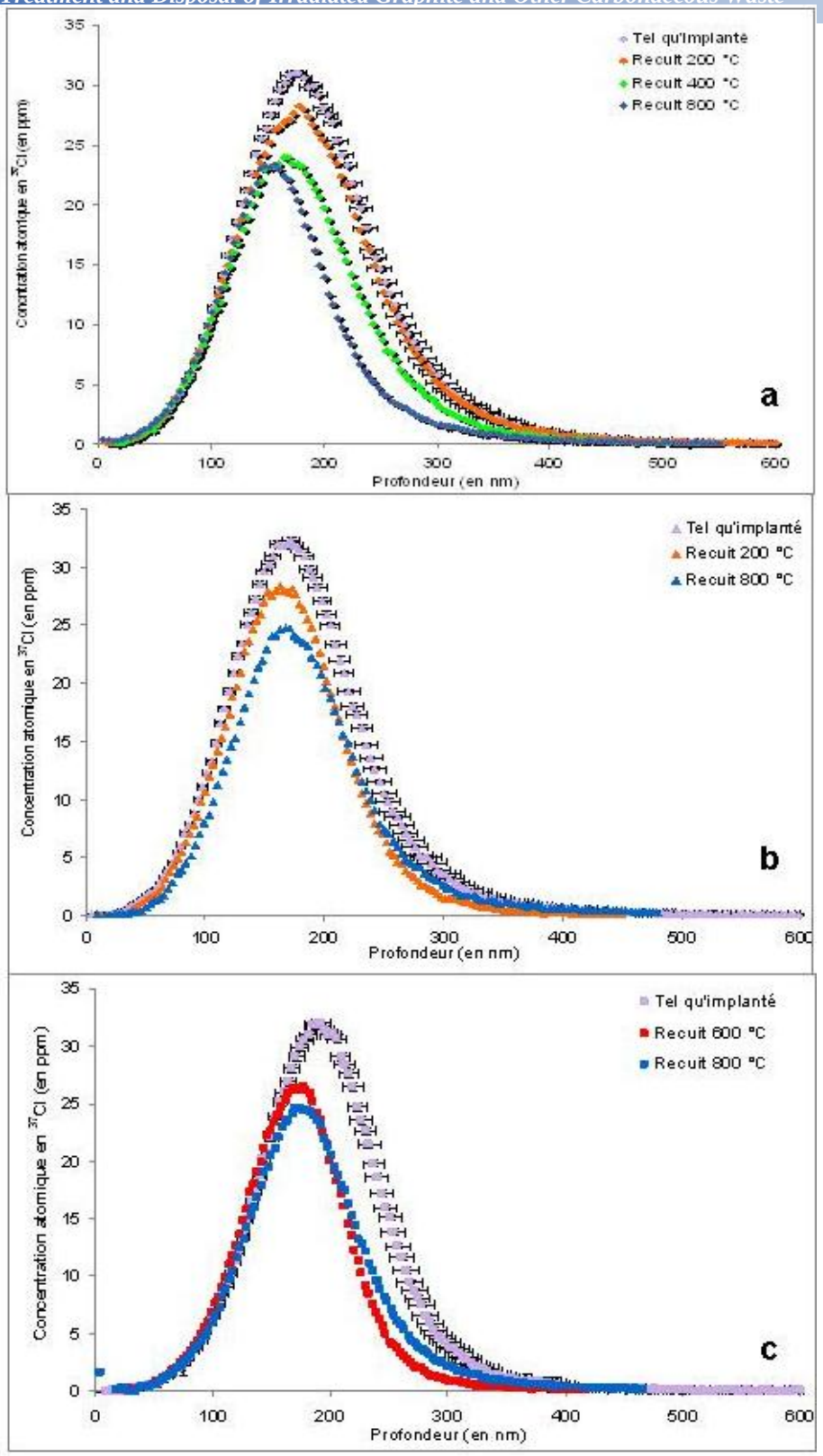

Figure 4-2 : Profiles of the concentration in ^{37}Cl, obtained by SIMS, for the samples of nuclear graphite from the (a) SLA2 sleeve for as-implanted samples and those annealed for 2 h at 200, 400 and 800 °C, (b) G2 reflector for as-implanted samples and those annealed for 2 h at 200 and 800 °C, and (c) i SLA2 moderator for as-implanted samples and those annealed for 4 h at 600 and 800 °C

Generally, we observed a decrease in the area under the chlorine profile at low temperatures (about 200 °C). However, in table 4-3, it can be seen that for the chlorine profiles of annealed samples there is no increase in the full width half maximum height (FWHM) and they are shifted, though the translation distance is accounted for in the measurement error.

Traitements subis par l'échantillon	FWHM (en nm)	Rp (en nm)
Tel qu'implanté	110	190 ± 15
Recuit 4 h à 200 °C	110	180 ± 20
Recuit 4 h à 400 °C	115	180 ± 20
Recuit 4 h à 600 °C	110	175 ± 20
Recuit 4 h à 800 °C	100	175 ± 20
Recuit 4 h à 1000 °C	105	210 ± 15

Table 4-3 : The FWHM and projected range (Rp) of the ^{37}Cl profiles for the SLA2 moderator samples for as implanted samples and those annealed for 4 h between 200 and 1000 °C

From these results, it is possible to say that no measurable diffusion or transport phenomenon exists. Between 200 and 1100 °C, for all the nuclear graphite studied, the principal migration mechanism of chlorine is thus diffusion and release. In this case, the general transport equation (4) in annex 6 is simplified and can be written in the following form:

$$\frac{\partial C(x,t)}{\partial t} = -k.C(x,t) \quad (1)$$

and its resolution becomes the following equation:

$$\frac{C_T}{C_0} = \exp(-k.\Delta t) \quad (2)$$

where C_T (in ppm) is the atomic concentration in ^{37}Cl present in a sample annealed at a temperature T, C_0 (en ppm) the atomic concentration of ^{37}Cl present in an as implanted sample, the kinetic release constant k in s^{-1} and the annealing time Δt in s.

In order to determine the kinetic release constant of chlorine, we present the evolution of the logarithm of the relation C_T/C_0 as a function of different annealing times at a temperature of 1100 °C for a sleeve sample from SLA2 (figure 4-3).

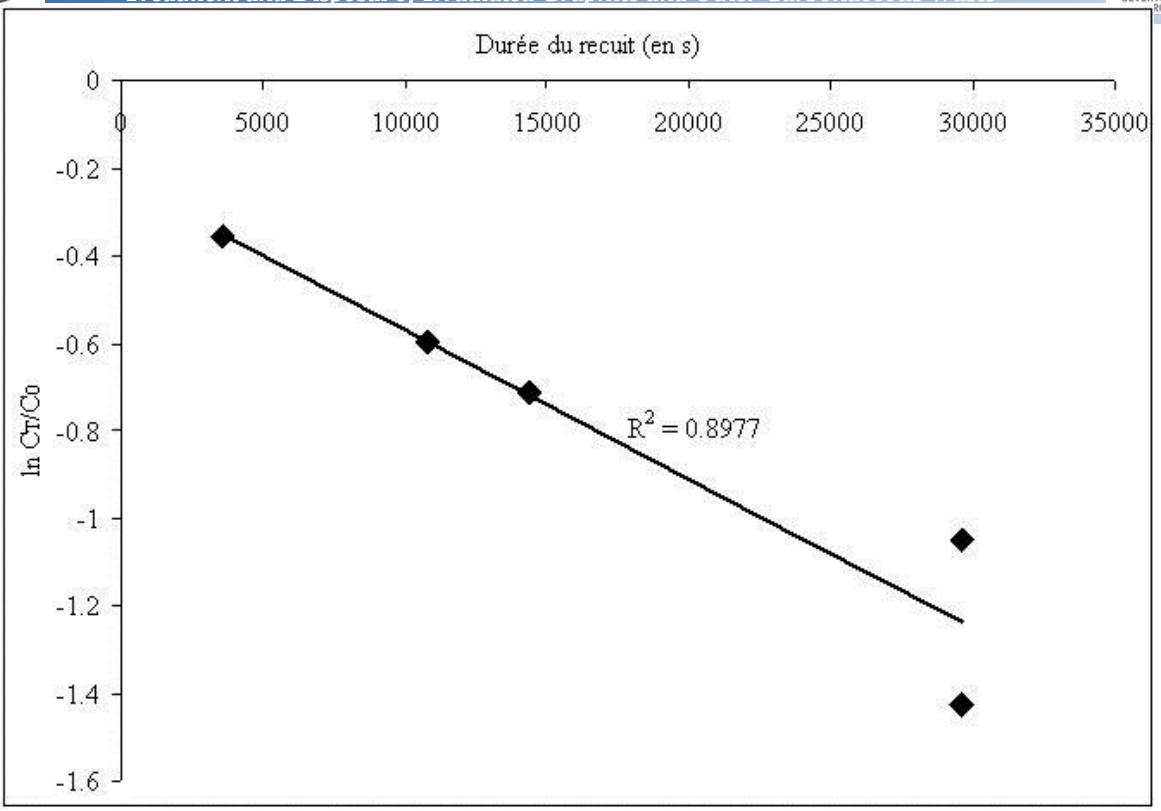

Figure 4-3 : Evolution of the logarithm of the relation C_T/C_0 as a function of the annealing times at a temperature of 1100 °C for a sleeve sample from SLA2

The approximation of our data to a straight line seems adapted as it has a correlation coefficient, R^2, equal to 0.8977. This correlation coefficient for straight line tendency corresponds to the release k of chlorine. In the case of graphite from the sleeve of SLA2, it is equal to $(3.40 \pm 0.66) \times 10^{-5}\ s^{-1}$.

Table 4-4 gathers together the values of the C_T/C_0 ratio, the percentage loss of ^{37}Cl and the release constant k measurements for the moderator samples from SLA2 with XY and Z orientations. (Note that the XY and Z samples, as well as the results obtained during their study, will be presented in paragraph A.I.2).a) of this report.) The values in table 4-4 were obtained at different temperatures for an annealing time of 4 h. For each sample, several measurements were taken at different positions. The errors on the C_T/C_0 ratios and k were calculated while taking into account the standard deviation of the distribution of the results.

The uncertainties in the C_T/C_0 ratio and k were calculated using the general formula (1) presented in annex 7. We observed that for an annealing time of 4 h, the percentage loss of ^{37}Cl increases as a function of the annealing temperature up to 800 °C. In fact, from this temperature, the loss of chlorine seems to stabilize and so reaches a plateau at about 30%. For longer annealing times (8 and 12 h) and a temperature of 800 °C, the percentage loss of ^{37}Cl is unchanged and remains equal to about 30%.

Température de recuit (en °C)	Echantillon	C_T/C_0	Relâchement en ^{37}Cl (en %)	Constante de relâchement k (en s^{-1})
200	XY	0,81 ± 0,19	18,8	(1,45 ± 1,85) x 10^{-5}
	Z	0,85	15,4	1,16 x 10^{-5}
400	XY	0,64 ± 0,17	35,6	(3,06 ± 1,66) x 10^{-5}
	Z	0,88 ± 0,03	11,8	(0,87 ± 0,30) x 10^{-5}
600	XY	0,70 ± 0,03	29,5	(2,43 ± 0,33) x 10^{-5}
	Z	0,81 ± 0,04	18,9	(1,45 ± 0,43) x 10^{-5}
800	XY	0,71 ± 0,02	29,0	(2,38 ± 0,22) x 10^{-5}
	Z	0,81 ± 0,13	19,4	(1,50 ± 1,26) x 10^{-5}
1000	XY	0,71 ± 0,17	28,9	(2,37 ± 1,70) x 10^{-5}
	Z	0,70 ± 0,11	30,3	(2,51 ± 1,52) x 10^{-5}

Table 4-4 : Loss of ^{37}Cl as a function of annealing temperature and for a time of 4 h, for moderator samples from SLA2

For all the nuclear graphite studied, the release activation energy could be estimated from the Law of Arrhenius (equation 3).

$$k = k_0 \exp\left(-\frac{E_a}{k_B.T}\right) \qquad (3)$$

where, the release constant, k, is in s^{-1}, the initial release constant, k_0, in s^{-1}, the activation energy, E_a, in eV, the Boltzmann constant, k_B = 8.65x10^{-5} eV K^{-1} and the annealing temperature, T, in K. Figure 4-4 is an Arrhenius diagram for chlorine release, i.e. a logarithmic representation of the release constant k as a function of the inverse of the annealing temperature, for nuclear graphite samples from the sleeve of SLA2, the reflector of G2 and the moderator of SLA2, respectively.

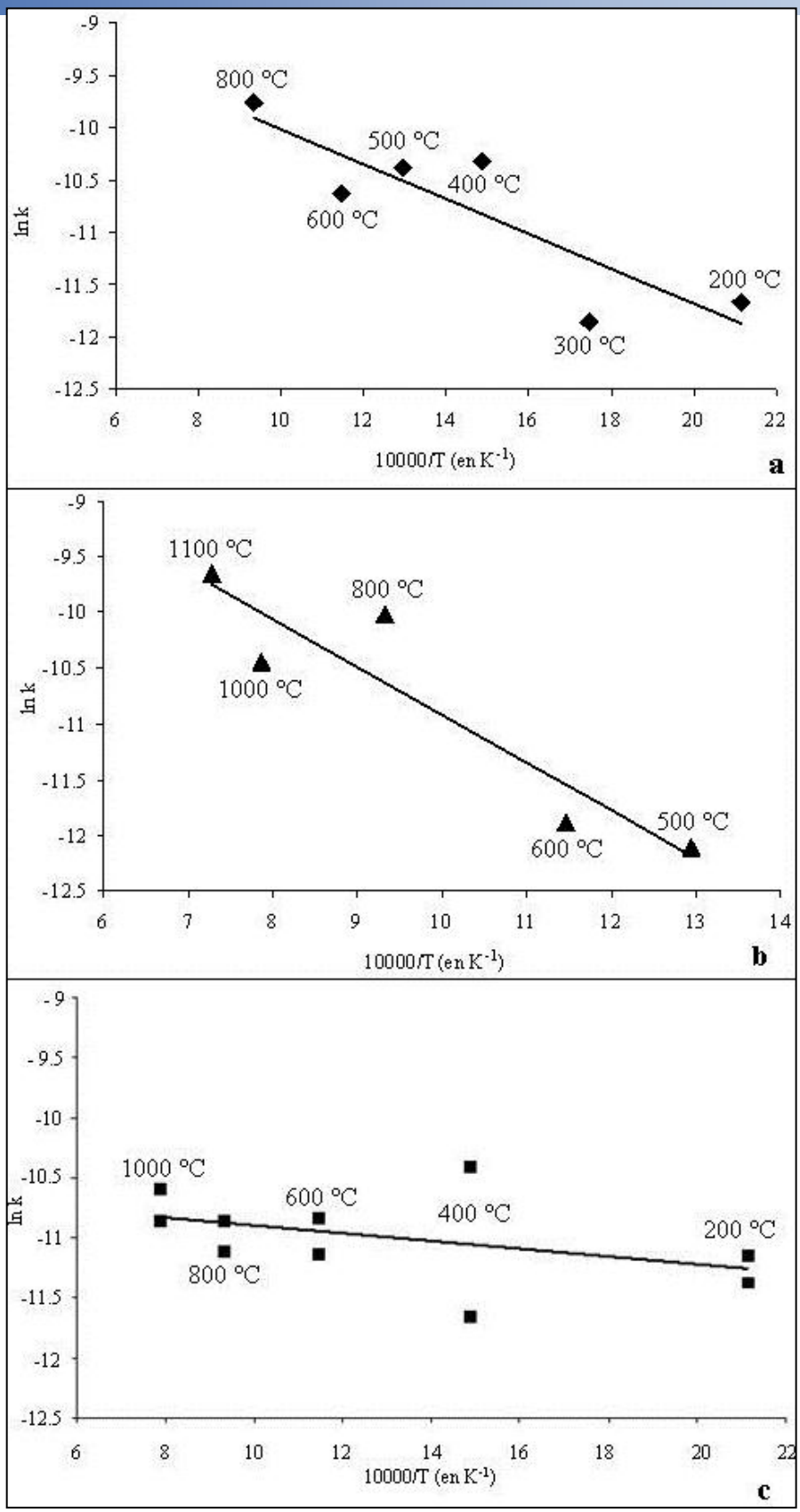

Figure 4-4 : Arrhenius diagram of chlorine release for nuclear graphite samples from (a) the SLA2 sleeve, (b) G2 reflector, and (c) SLA2 moderator

The correlation coefficients for the straight lines enable us to calculate the activation energies for release of ^{37}Cl. They are 0.14 ± 0.04 eV, 0.37 ± 0.09 eV and 0.03 ± 0.03 eV, for the SLA2 sleeve, G2 reflector and SLA2 moderator, respectively. For all the nuclear graphites analyzed, the activation energy for release of ^{37}Cl is therefore below 0.50 eV. Given that thus value is very low, the release of chlorine can be considered as quasi-athermal which explains that a part of the chlorine is extremely mobile in the nuclear graphite.

In order to determine if the chlorine release is accompanied by a modification of its distribution in the graphite matrix, we analyzed, by SIMS in image mode, a sample of nuclear graphite from the G2 reflector annealed at 800 °C during 2 h. Figure 4-5 presents a mapping of the implanted chlorine (^{37}Cl) for this sample. To obtain a signal from ^{37}Cl of a maximum intensity, this mapping was realized at a depth corresponding to the maximum implantation profile, i.e. 180 nm in the case of the reflector.

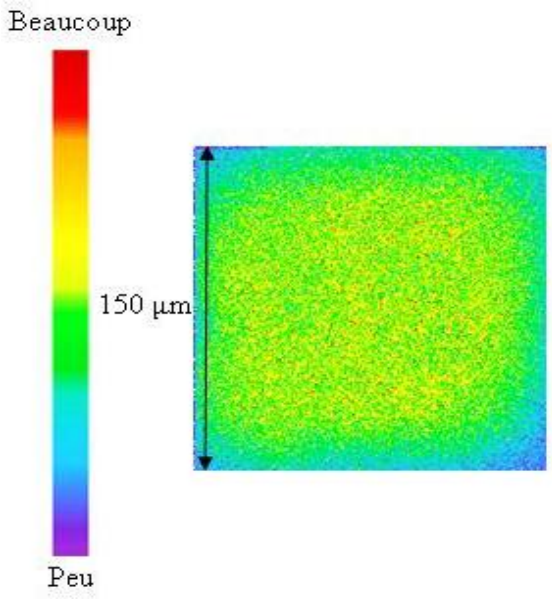

Figure 4-5 : SIMS mapping of ^{37}Cl for a sample of nuclear graphite from the reflector of G2 annealed at 800 °C during 2 h

We observed that the distribution of implanted ^{37}Cl at a fluence of $5x10^{13}$at.cm^{-2} remains homogeneous during thermal treatment. This result is contrary to that of the thermal behavior study of implanted chlorine at a fluence of $1x10^{13}$at.cm^{-2} in uranium dioxide [Y. Pipon 2006], where no re-concentration of chlorine in the form of clusters was observed.

A.I.2) Effect of porosity and structural orientation of graphite

In order to evaluate the effects of porosity and structural orientation of graphite in the release of chlorine, we studied two types of graphite: nuclear graphite from the moderator of SLA2 presenting preferential orientations, and non-porous and very orientated monocrystalline HOPG (Highly-Oriented Pyrolytic Graphite), the "model" graphite.

A.I.2).a) Nuclear graphite

Two preferential orientations of the grains in the SLA2 moderator were examined. The two samples were taken from the same moderator of graphite as illustrated in figure 4-6.

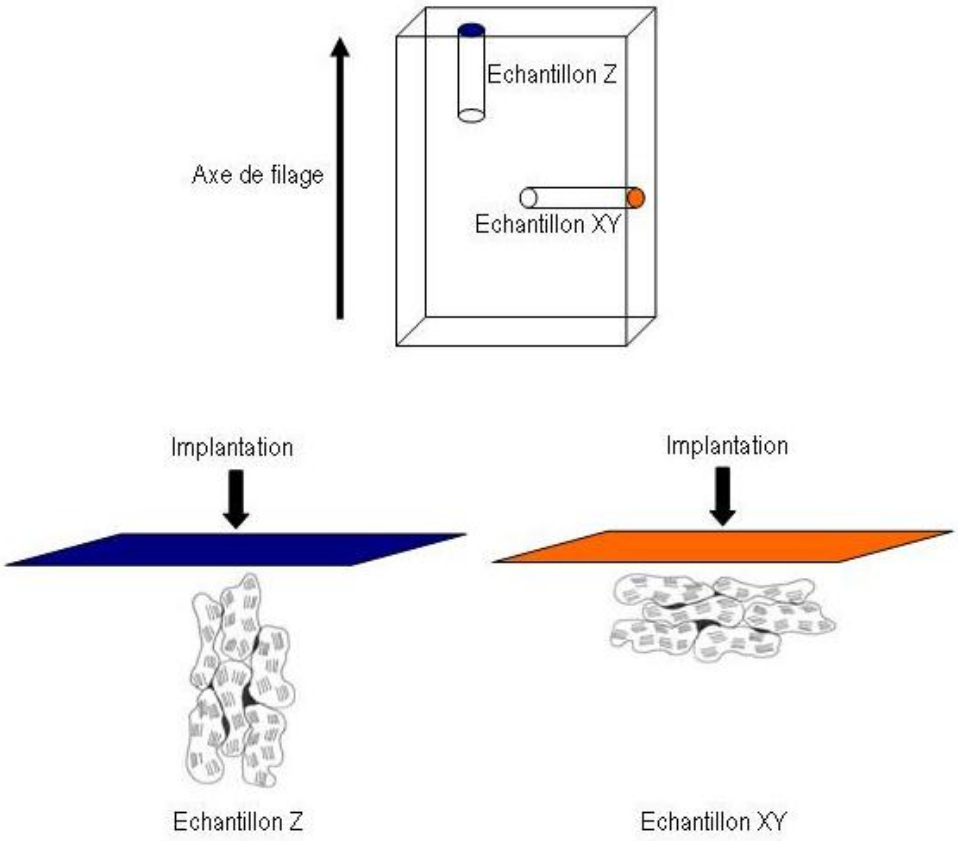

Figure 4-6 : Diagram showing the sample grains of the SLA2 moderator graphite with XY and Z orientations, as well as the direction of ^{37}Cl implanting

The sample marked Z had been implanted with ^{37}Cl along the extrusion axis, whereas the other, called XY, had been implanted perpendicular to this axis. Sample Z contains grains which are preferentially oriented along the extrusion axis, whereas sample XY contains grains which are preferentially oriented perpendicular to this axis. In addition, sample XY has more accessible pores than sample Z. Figure 4-7 shows the as-implanted ^{37}Cl profiles for samples XY and Z.

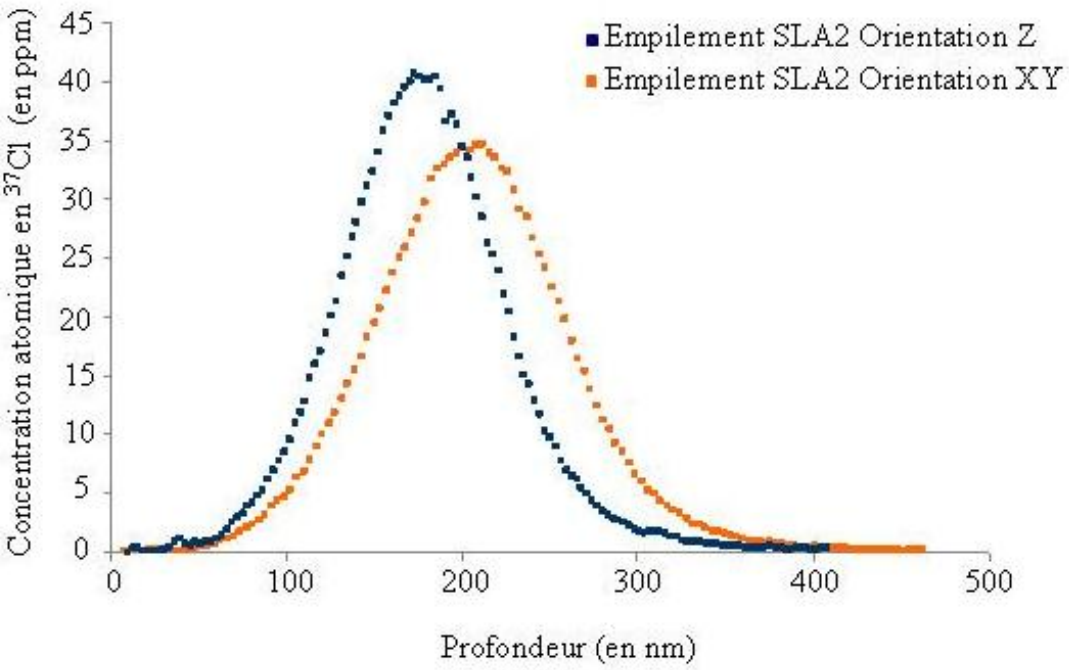

Figure 4-7 : Profiles of as-implanted ^{37}Cl for the XY and Z samples

From this figure, it is possible to see the differences between the two as-implanted ^{37}Cl profiles. In fact, even if the two profiles are Gaussian in shape, the implanted peak is broader at the bottom in the case of the XY sample, even though the latter has more accessible pores than the Z sample. It therefore appears that the porosity of the graphite constitutes a preferential pathway for the implanting of ^{37}Cl. Figure 4-8 shows the loss of ^{37}Cl after 4 h of annealing as a function of temperature for the XY and Z samples.

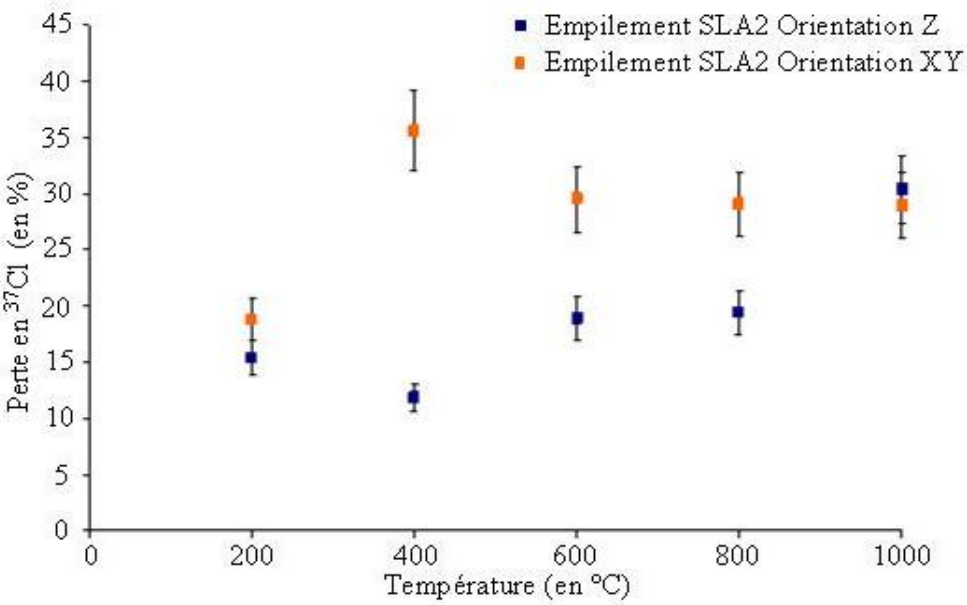

Figure 4-8 : Loss in ^{37}Cl after 4 h of annealing, as a function of temperature for the XY and Z samples

This figure reveals the different chlorine release rates for each of the samples. In fact, at a given temperature and after 4 h of annealing, the release of chlorine is greater for sample XY than for Z.

Figure 4-9 presents the Arrhenius diagrams for the release of ^{37}Cl, for the XY and Z samples. We can observe that for these samples, the activation energies for the release of ^{37}Cl are 0.01 ± 0.01 and 0.04 ± 0.02 eV, respectively. This slight difference can be explained by the fact that the XY sample has more accessible pores than Z; the activation energy necessary to initiate the release of ^{37}Cl is therefore lower for the former.

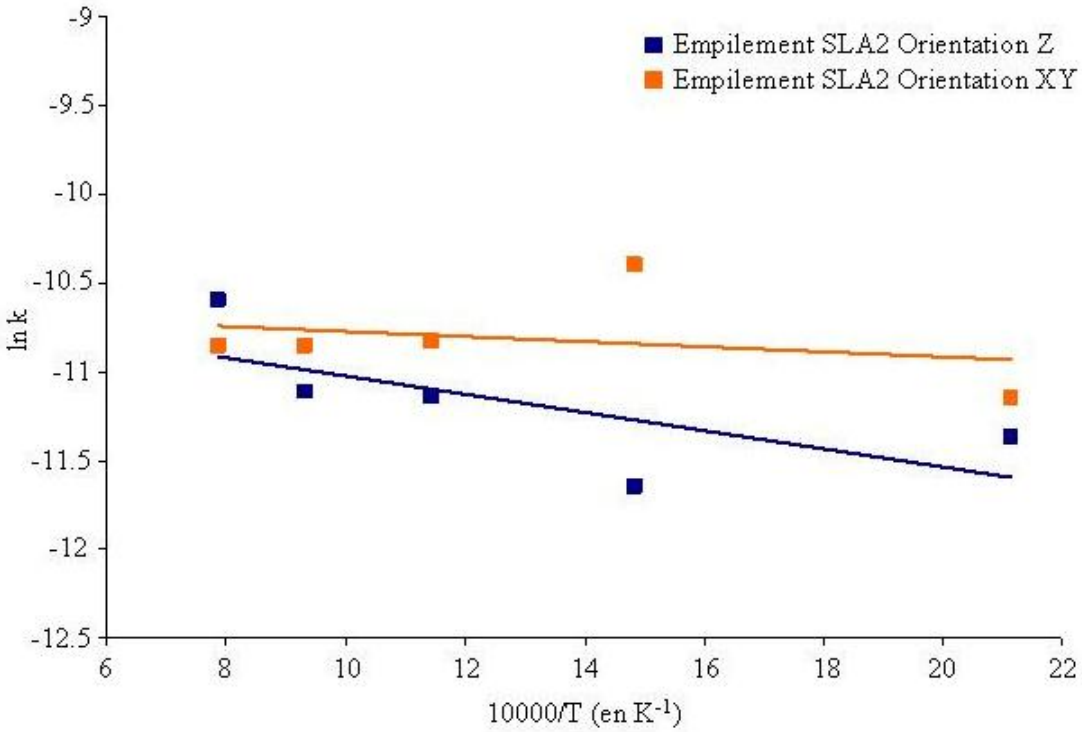

Figure 4-9 : Arrhenius diagram of ^{37}Cl release for the XY and Z samples

All of the results obtained illustrate the fact that porosity seems to constitute a preferential pathway for the release of chlorine.

A.I.2).b) "Model" graphite

To evaluate the effects of porosity and to focus on the role of the structural orientation of the graphite, we have studied a "model" graphite. Its mass volume is 2.27 g cm^{-3} because it is not porous. In addition, it has an extremely oriented structure, as much on the scale of the graphene planes, as that of the grains [SPI Supplies; Chapter 2.I.1)].

As in the case of nuclear graphite, two orientations of the HOPG were examined. Figure 4-10 shows the orientation of the graphene planes within each of the samples, as well as the direction of implanting of ^{37}Cl. The sample denoted Z' was implanted parallel to the graphene planes. Conversely, the sample XY', was implanted perpendicular to the graphene planes. It is

important to point out that the implanting conditions are the same as those chosen for nuclear graphite [Chapter 3.I.2).b)].

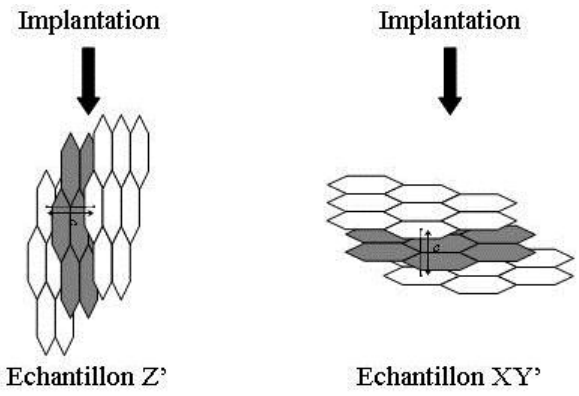

Figure 4-10 : Diagram showing the graphene planes in the HOPG samples with XY' et Z' orientations, as well as the direction of the ^{37}Cl implanting

The results obtained from HOPG with orientation Z' cannot be used. In fact, as can be seen in the SEM (Scanning Electron Microscope) image, (figure 4-11), the majority of the surface studied is not a stack of graphene planes but rather a layer, or a thickness of about 1 µm, of disorganized carbon atoms. This artifact results from the inevitable bending of the graphene planes during the sample cutting step.

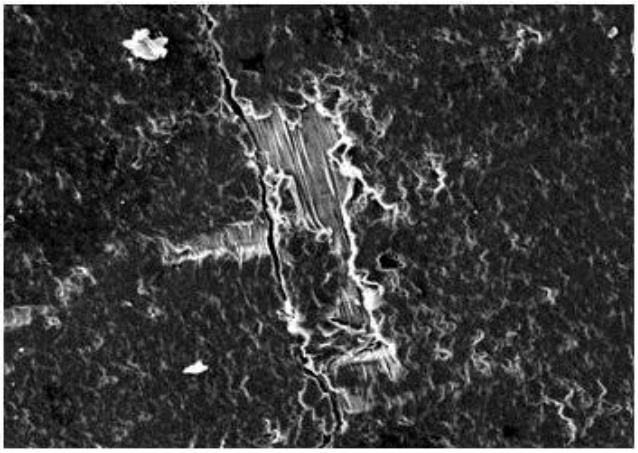

Figure 4-11 : MEB Image of an HOPG Z' sample

For the HOPG XY' samples, figure 4-12 shows the quantity of chlorine released as a function of the annealing temperature. In a temperature range between 200 and 1000 °C and for an annealing time of 4 h, it seems that the chlorine release is very small. This result can be explained by the lack of porosity in HOPG.

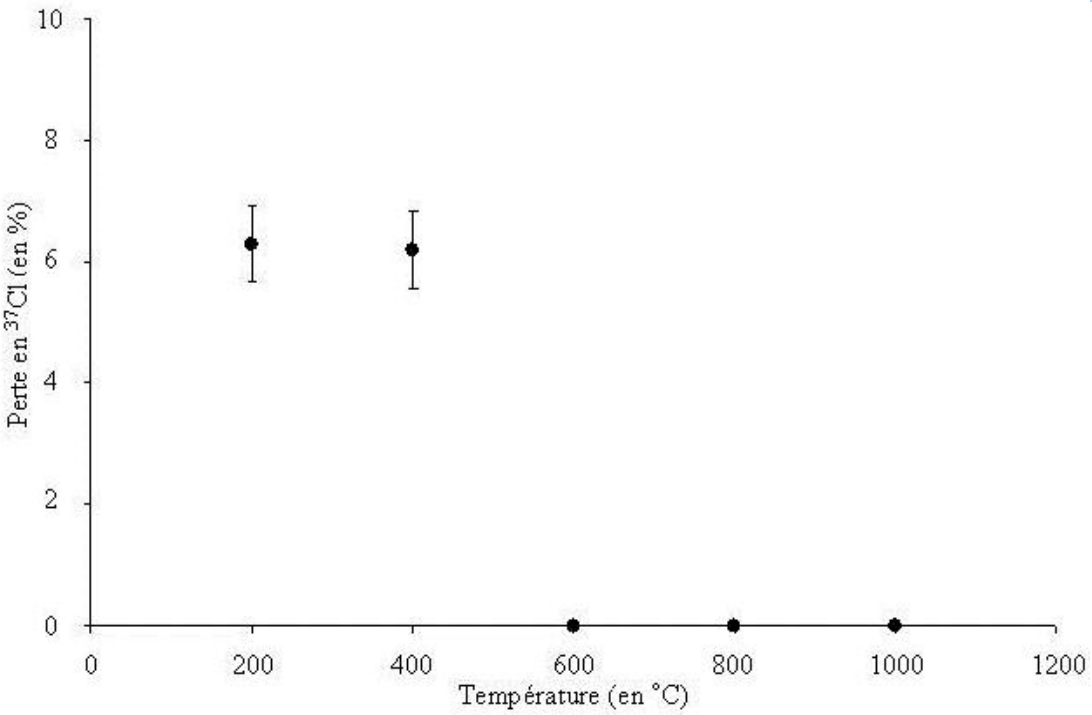

Figure 4-12 : Loss in ^{37}Cl, after 4 h of annealing, as a function of temperature for the HOPG XY' samples

A.I.2).c) Conclusion

These studies of nuclear graphite and "model" graphite have enabled us to show the importance of the effects of texture and structural orientation of a matrix on the migration mechanism of an impurity, such as chlorine. We have highlighted the role played by the graphite pores on the release of chlorine. In fact, the pores in the matrix constitute preferential pathways for the chlorine. In the case of nuclear graphite, chlorine is therefore principally released due to the porosity of the material.

A.II Following the evolution of the graphite structure using Raman microspectroscopy

The evolution of the nuclear graphite sample structure (from the SLA2 sleeve, G2 reflector and SLA2 moderator) and the "model" graphite (HOPG) was followed by Raman microspectroscopy at each step of the experimental protocol [Chapter 3.III.2).a)]. The spectra obtained for all the samples are presented in figures 4-13 and 4-14. Each spectrum represents the average of two to six spectra. In order to compare them, they have been normalized with respect to band G of the graphite.

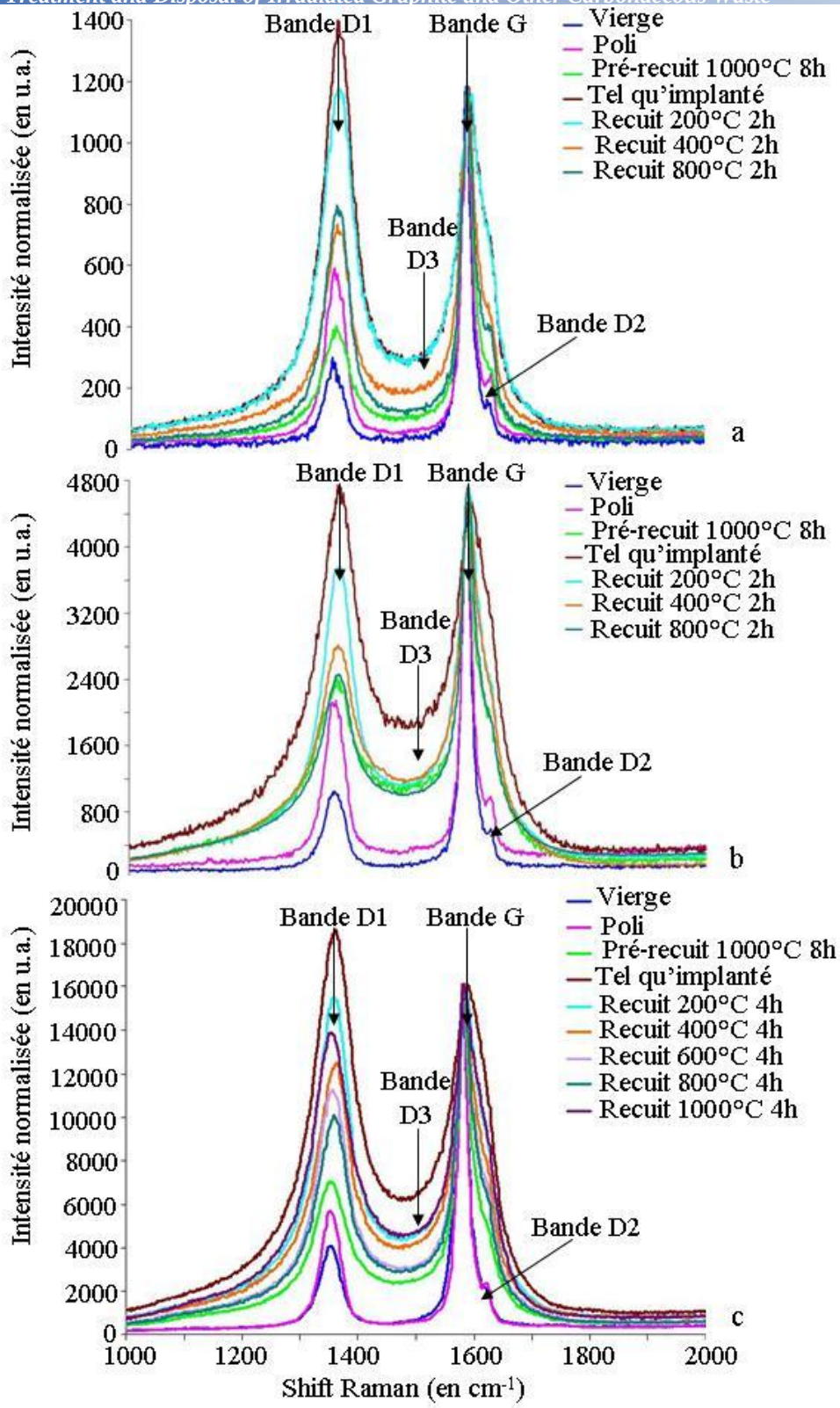

Figure 4-13 : Raman spectra of (a) the SLA2 sleeve, (b) G2 reflector and (c) SLA2 moderator realized at the end of each step of the experimental protocol

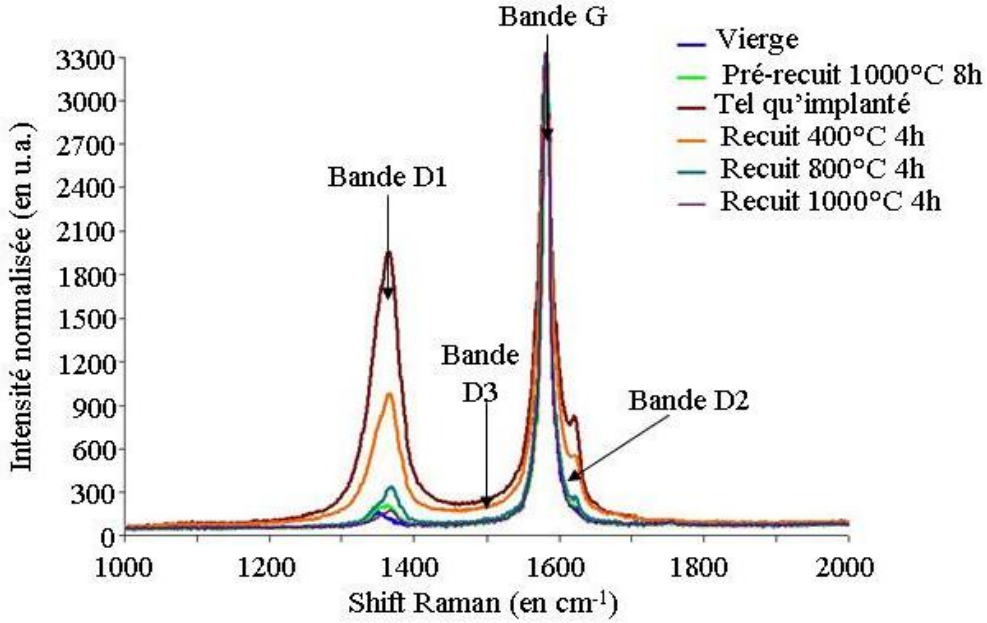

Figure 4-14 : Raman spectra of HOPG realized at the end of each step of the experimental protocol

In the case of virgin nuclear graphite, three Raman bands, G, D1 and D2, were observed. Band G, at 1580 cm^{-1}, is called the graphitization band. The narrower and more intense it is, the more the graphite has been well-graphitized. The presence of two defect bands, D1 and D2, indicates that the nuclear graphite is not perfectly well-structured. Band D1, at 1350 cm^{-1}, correlates to the size of the crystallites. Band D2, at 1620 cm^{-1}, is associated with the distribution of the dimension of the interplanar spaces [J. N. Rouzaud et al. 1983; A. Sadezky et al. 2005]. In the case of virgin HOPG, only two Raman bands, G and D1, were identified. The absence of band D2 and the low intensity of band D1 illustrate the fact that the virgin HOPG, contrary to virgin nuclear graphite, has only a few defects.

We will now discuss the effects of the different steps of the experimental protocol on the evolution of the graphite structure.

Polishing induces an increase in the intensities of bands D1 and D2 (see figures 4-13 and 4-14), which signifies that the size of the crystallites decreases and that the distribution of the dimension of the interplanar space increases [M. Nakamizo and K. Tamai 1984]. The samples ate therefore altered by the polishing step, even if this is done manually.

In order to characterize the effect of pre-annealing at 1000 °C during 8 h on the evolution of the graphite structure and to complete the data obtained by Raman microspectroscopy, we analyzed the samples of nuclear graphite and HOPG by SIMS in profilometry mode. Figure 4-15 presents the ^{12}C profiles, obtained by SIMS, for two SLA2 sleeve samples: one polished, the other, polished and pre-annealed at 1000 °C during 8 h and for two samples of HOPG: one virgin, the other, pre-annealed at 1000 °C during 8 h. In the case of the nuclear graphite samples (figure 4-15a), the carbon signal only stabilizes after 650 s of etching for the polished sample and not pre-annealed. For the pre-annealed samples, this stabilization occurs after 100 s of etching. On the contrary, in the case of the HOPG sample which has not been polished (figure

4-15b), the pre-annealing plays no role in the stabilizing the carbon signal. These data show that pre-annealing enables the removal of some of the polishing defects.

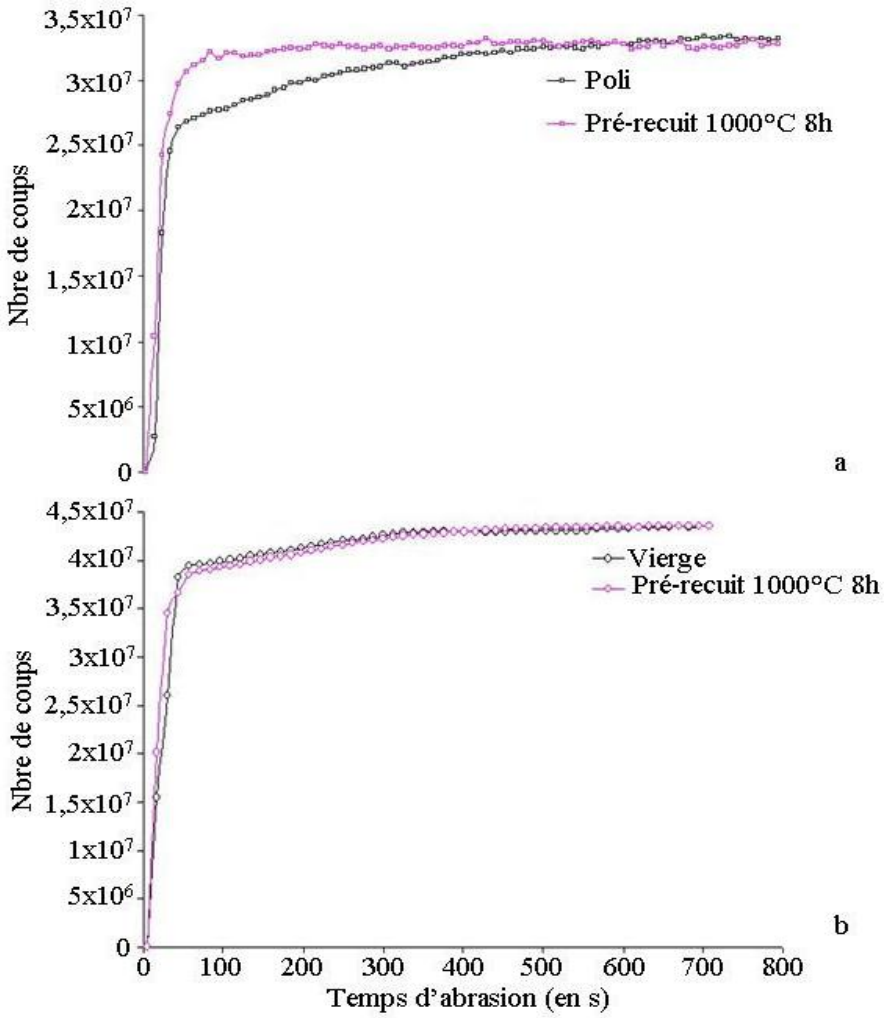

Figure 4-15 : ^{12}C profiles obtained by SIMS for (a) two SLA2 moderator samples: one polished, the other polished and pre-annealed at 1000 °C during 8 h and (b) two HOPG samples: one virgin, the other pre-annealed at 1000 °C during 8 h

Implantation induces a clear modification of the Raman spectra of the different graphites studied (see figures 4-13 and 4-14). All the bands broaden and their intensities increase. The significant growth of band D1 is related to the fact that the implanted chlorine breaks the crystallites and induces a decrease in their size. The appearance of the intense and wide band D3 is symptomatic of an amorphous state. In fact, during the implanting, the bonds between the sp^2 hybrid carbon atoms of the aromatic rings are broken and the bonds between carbon atoms of the different graphene planes form. Therefore, both sp^2 and sp^3 hybrid carbons exist [B. S. Elman et al. 1982]. The implanting of ^{37}Cl, even at a relatively low fluence ($5x10^{13}$ at cm^{-2}), therefore generates defects (total number of defects created in the implanted zone equals 0.5 dpa) which appear in the form of vacancies and interstitials in and between the graphene planes [T. Tanabe et al. 1995]. At the end of this step of the experimental protocol, the samples are thus destructured.

For all the samples studied, annealing induces, below a temperature of 200 °C, a decrease in the intensity of the defect bands and a narrowing of the G band (see figures 4-13 and 4-14). The thermal treatment therefore enables the materiel to be restructured [J. N. Rouzaud et al. 1983; B. S. Elman et al. 1982]. With annealing, the vacancies and interstitials recombine. In addition, certain interstitials move into the pores and the grain boundaries [T. Tanabe et al. 1995]. This tendency continues with the increase in annealing temperature but does not allow the initial structure of the graphite to be recovered (see figures 4-13 and 4-14). This result is coherent with those obtained by T. Tanabe and his team. In fact, they showed that, in general, a carbon-containing material which has been submitted to more than 0.1 dpa does not recover its initial structure for annealing temperatures below 750 °C [T. Tanabe et al. 1995]. In the case of nuclear graphite samples, the restructuring of the graphite matrix seems to correlate to the release of chlorine [Chapter 4.A.I.2).a)]. However, in the case of HOPG, the matrix is restructured even though only a small release of chlorine is observed [Chapter 4.A.I.2).b)]. In the two cases, the thermal treatment induces, on the one hand, a more uniform distribution, together with a decrease in the distance between the graphene planes, and on the other hand, an increase in the size of the crystallites. The release of chlorine, if the latter is found between the graphene planes, frees the space between these planes and therefore seems to be able to facilitate the restructuring of the graphite. Nevertheless, only the effect of temperature is necessary to initiate the restructuring of the material because in the case of HOPG, we observed a restructuring of the matrix even though only a negligible quantity of chlorine is released. Similar results were obtained by B. S. Elman and his team [B. S. Elman et al. 1982]. They proved that thermal treatment of HOPG decreases the interplanar distance and thus triggers the release of impurities between the graphene planes, when the diameter of the impurity is greater than this distance.

The study of the evolution of the graphite structure during different steps of the experimental protocol allowed us to anneal the damage caused by the polishing, and especially, by ionic implanting. Moreover, it has been shown that a partial restructuring of the graphite matrix is induced by this thermal treatment.

These data could be extrapolated to the evolution of the nuclear graphite structure during its time in the reactor. In fact, the structure of the graphite is, on the one hand damaged when bombarded by neutrons [Chapter 2.I.4).a)] and on the other, reorganized under the effect of temperature [Chapter 4.A.II]. In the reactor, the neutron flux profile is hyperbolic and reaches its maximum at the centre of the moderator [F. Bérenger 2007]. As a consequence, the graphite moderator is destructured at its greatest at the centre of the reactor and minimal at the peripheral part. Concerning the temperature, that of graphite is between 100 and 500 °C as long as it is situated in the high or low part of the reactor [Chapter 1.I.2).b).i]. It is therefore necessary to wait to observe a restructuring gradient of the matrix as a function of the height. In the reactor, the joint action of the neutron flux and temperature without doubt leads to a very destructured matrix in the high and central parts of the moderator, whereas there is little damage in the low and peripheral parts.

A.III Follow-up of the evolution of the quantity of oxygen in nuclear graphite by nuclear backscattering spectrometry (NBS)

We have also realized a follow-up of the evolution of the quantity of oxygen in the samples of nuclear graphite during the different steps of the experimental protocol. In fact, oxidation can

lead to a change in the stœchiometry of a sample. The migration mechanism of chlorine is therefore studied in graphite where the stœchiometry is no longer representative of the non-oxidized material.

The quantity of oxygen in the different samples was measured on the 4 MV accelerator of the IPNL by nuclear backscattering spectrometry using the reaction ^{16}O (α, α') ^{16}O [Chapter 3.III.1).b)]. Tables 4-5 and 4-6 present the results obtained for the nuclear graphite samples of the sleeve and the moderator of SLA2.

Traitements subis par l'échantillon	Quantité d'oxygène (en 10^{15} at cm^{-2})
Vierge	14 ± 1
Poli	56 ± 1
Pré-recuit 1000 °C 8h	6 ± 1
Tel qu'implanté	10 ± 1
Recuit 200 °C 2h	9 ± 1
Recuit 400 °C 2h	9 ± 1
Recuit 600 °C 2h	9 ± 1
Recuit 800 °C 2h	9 ± 1

Table 4-5: Quantity of oxygen in the SLA2 sleeve samples after being submitted to different treatment

Traitements subis par l'échantillon	Quantité d'oxygène (en 10^{15} at cm^{-2})
Vierge	23 ± 1
Poli	24 ± 1
Pré-recuit 1000 °C 8h	23 ± 1
Tel qu'implanté	22 ± 1
Recuit 400 °C 4h	12 ± 1
Recuit 1000 °C 4h	19 ± 1

Table 4-6: Quantity of oxygen in the SLA2 moderator samples after being submitted to different treatment

The SLA2 virgin moderator (see table 4-6) contains almost double the amount of oxygen as the SLA2 virgin sleeve (see table 4-5). This difference can be explained by the synthesis step of the as-implanted nuclear graphite [Chapter 2.I.2).d).iii]. In fact, the moderator underwent only one impregnation, contrary to the sleeve which had two. Consequently, the moderator samples are more porous and therefore offer a greater quantity of internal surfaces accessible to the oxygen than that of the sleeve. Nevertheless, the evolution in the quantity of oxygen present in the samples during the different steps of the experimental protocol is similar.

Polishing, however, leads to an increase in the quantity of oxygen. In the case of the SLA2 sleeve, the amount of oxygen present after polishing is four times greater than that contained in a virgin sample. This difference can perhaps be linked to the adsorption of OH functions at the surface of the graphite during the polishing which is done in the presence of ethanol [Chapter 3.I.1)]. Annealing [Chapter 3.II.1)] leads to desorption of OH and the residual water on the graphite, and as a consequence leads to a decrease in the quantity of oxygen present in the samples.

These results allow us to conclude that whatever the type of graphite studied the experimental protocol used does not lead to an oxidation of the surface of the samples which could have biased the study of the chlorine migration in nuclear graphite.

A.IV Conclusion

This study has enabled us to identify the principal mechanism of migration of chlorine in nuclear graphite. Under the effect of thermal treatment, chlorine is released, and this from a temperature of 200 °C. The activation energy of this process is low as it is below 0.50 eV for all the nuclear graphites studied. Part of the chlorine is therefore extremely mobile in the graphite, though it is important to point out that different activation energies were obtained for the SLA2 sleeve, the G2 reflector and the SLA2 moderator. It is difficult to explain the origin of this difference but it is perhaps linked to the nature of the graphite and so the raw material used during its synthesis (petroleum coke, coal tar pitch, purifying agent).

At 500 °C, the maximum temperature of the graphite in the reactor, and for short annealing times (4 h) the chlorine concentration is reduced by about 20 %. For the same time of annealing but at higher temperatures (800 and 1000 °C) the loss of chlorine reaches a plateau at about 30 %. We have also shown that at 800 °C, for longer annealing times (8 and 12 h), the loss of chlorine peaks and then flattens out at about 30 %. These results are in agreement with those obtained by A. M. Clayton and his team, on nuclear graphites destined to be used in AGRs (Advanced Gas-cooled Reactors) [A. M. Clayton et al. 1996]. For their samples annealed at 500 °C for 4 and 11 h, the authors showed that the loss of chlorine, measured by neutron activation, was in the order of 40 %. It is necessary to anneal for 27 h at 500 °C to be able to observe an increase in the loss of chlorine which is then equal to 50 %.

Wue to the effect of thermal treatment, it seems that chlorine is released from nuclear graphite with two kinetic rates: fast then slow. In order to acquire data on the slow kinetics of chlorine release, one objective of our study was the realization of a series of annealings at 800 °C for long annealing times (30, 40 and 50 h). Consequently, these results prove that a significant quantity of chlorine is probably released in the coolant gas very soon after the start-up of the reactor.

In this study, we have also highlighted the role of the graphite structure in the chlorine release mechanism. In the case of a porous graphite (nuclear graphite), the chlorine starts to be released at a temperature of 200 °C, whereas in the case of non-porous graphite (HOPG) there is little or no release until 1000 °C. In the range of times and temperatures studied, the chlorine release therefore occurs principally because of the porosity of the material.

Finally, we have obtained data about the evolution of the nuclear graphite structure during its time in the reactor. In fact, it is submitted to the joint actions of the neutron flux and

temperature which means we obtain a material which is highly destructured in the upper and central parts of the moderator and little damaged in the lower and peripheral parts, in the case where the coolant gas circulates from top to bottom of the reactor.

B. Thermal behavior of constitutive chlorine

The data obtained in this study concern, on the one hand, the characterization of the constitutive chlorine distribution and the identification of its speciation in the virgin nuclear graphite, and on the other hand, the detection of the gaseous species desorbed from the graphite and the evolution of the chlorine speciation under the effect of thermal treatment. To realize this study, we used the following experimental protocol: firstly, after having cut the samples, we annealed some of them, during 4 h at 200, 600 or 1000 °C in order to study the effect of the thermal treatment on the behavior of the constitutive chlorine of nuclear graphite. Secondly, we analyzed the samples using different techniques. The distribution of constitutive chlorine in the virgin nuclear graphite was characterized by an ionic microprobe in image mode. The effect of thermal treatment on the graphite matrix was studied by helium pycnometry and thermal analyses. Finally, photoelectron and X-ray absorption spectroscopy allowed us to follow the evolution of the speciation of the constitutive chlorine under the effect of thermal treatment. The schematic presentation of the experimental protocol used is given in figure 4-16.

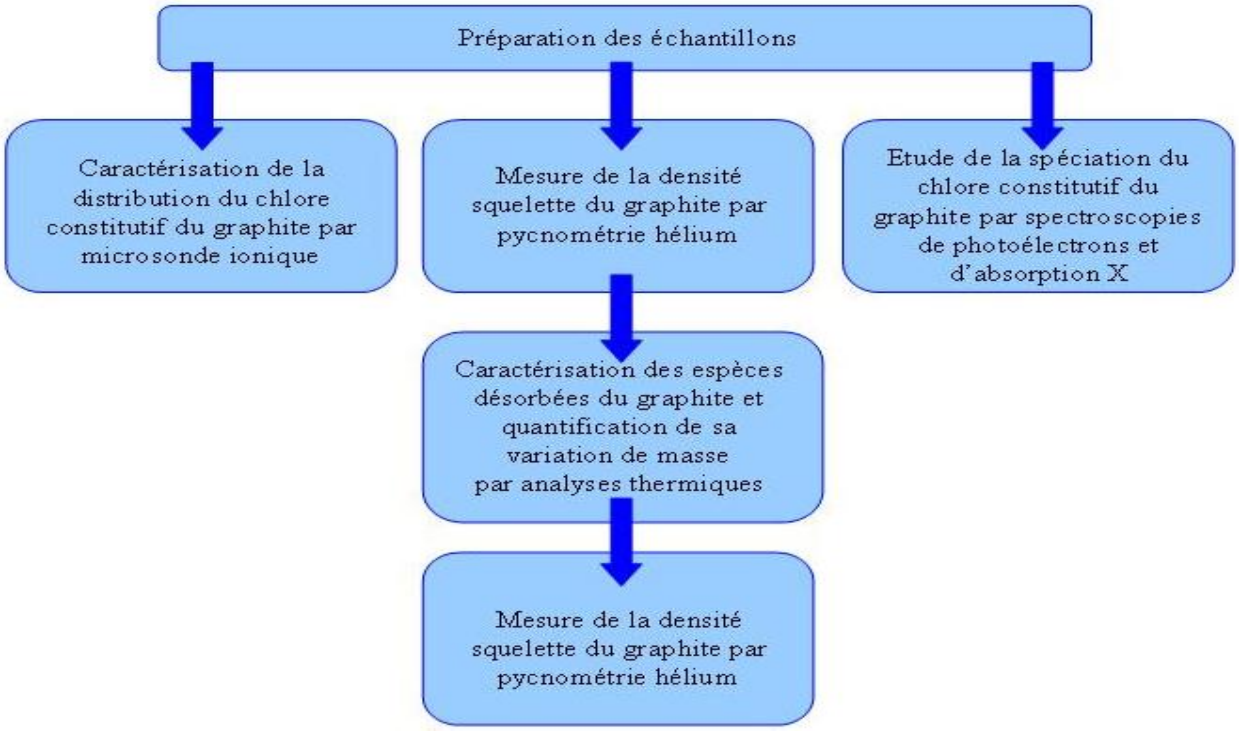

Figure 4-16 : Schematic representation of the experimental protocol used for the study of the thermal behavior of constitutive chlorine in nuclear graphite

B.I Constitutive chlorine distribution

We wanted to study the distribution of constitutive (naturally-occurring) chlorine and oxygen in the nuclear graphite in order to show an eventual correlation between the distribution of these impurities and the structure of the matrix. Virgin nuclear graphite samples from the G2 reflector and SLA2 moderator were analyzed by SIMS in image mode [Chapter 3.III.1).a).iii; L. Raimbault 2009]. In addition, to remove the surface pollution, principally due to adsorption of atmospheric gases, the samples were etched to a depth of about 40 nm before doing the mapping [Chapter 3.III.1).a).iii]. However, it was nevertheless difficult to obtain ionic images of satisfactory quality. In fact, the topographic irregularities of the surface of the samples neighboring the analyzed zones led to ion loss and so also to loss of information. This phenomenon is particularly exacerbated at the edge of craters and therefore at the edge of the ionic images. Nevertheless, figure 4-17 shows a mapping of constitutive oxygen (^{16}O) and chlorine (^{35}Cl), as well as the corresponding optical image obtained for the two types of virgin graphites cited above.

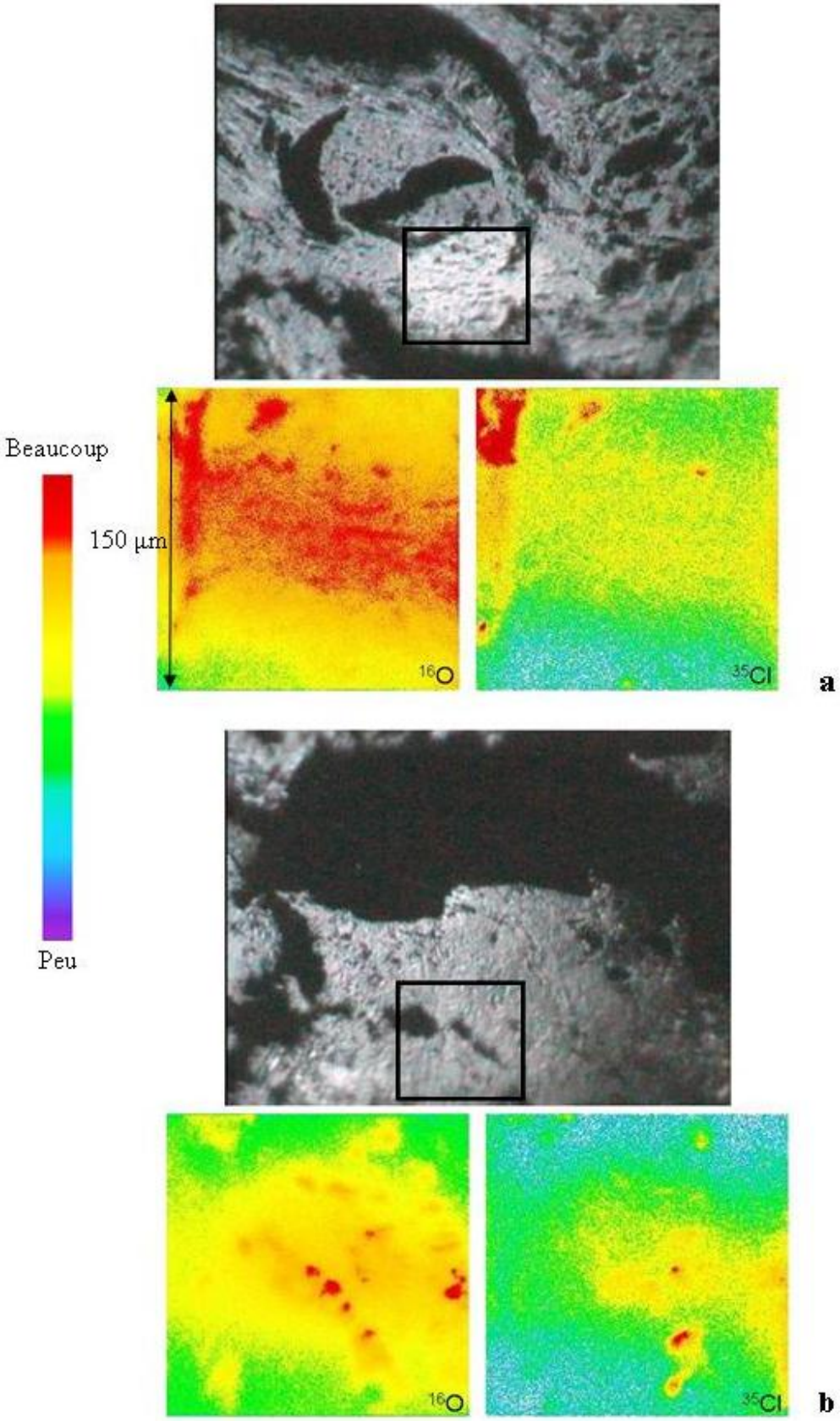

Figure 4-17 : The SIMS mapping of ^{16}O and ^{35}Cl with the corresponding optical image (indicated by the black squares) for virgin nuclear graphite from the (a) G2 reflector and (b) SLA2 moderator

As can be seen from this figure, these ionic mapping were realized on a square surface (sides of 150 µm). It clearly shows that the chlorine enriching does not correlate with that of oxygen. The zones enriched in oxygen correspond to a preferential east-west orientation of the graphite structure observable on the optical image of the G2 reflector sample (figure 4-17a). For the SLA2 moderator sample (figure 4-17b), the series of aligned points indicating the enriched oxygen correlates to the porosity seen on the optical image. In the case of the virgin nuclear graphite, it therefore seems that the heterogeneity of the distribution in oxygen can be linked to the porosity of the matrix. For the two types of nuclear graphite studied (figure 4-17), chlorine presents a heterogeneous distribution characterized by accumulation points of very small size. Nevertheless, it is impossible to determine the size of these clusters of chlorine as they are smaller than the spatial resolution of our apparatus i.e. 4 ± 1 µm. The occasional zones enriched in chlorine could correspond, either to nano-crystals of chlorides, or the clusters, whose size can attain that of micrometers. Nevertheless, it probably does not concern the accumulation of oxides as the enriching in chlorine does not correlate with that of oxygen.

B.II Nature of the gaseous species released during thermal treatment

Using programmed thermal desorption (TDP), we have studied the chemical forms in which the chlorine is likely to be released at different temperatures. These experiments were realized between ambient temperature and 800 °C on samples of virgin graphite from the SLA2 sleeve, G2 reflector and SLA2 moderator [Chapter 3.II.2).a)]. In the case of the SLA2 moderator, the study was done for two preferential orientations of the grains by using XY and Z samples [Chapter 4.A.I.2).a)]. Before carrying out all the experiments, we realized a "blank test" which ensured that the desorbed species did not come from the degassing of the experimental system.

B.II.1) Desorption of oxygenated species and hydrogen chloride

Five gaseous oxygen-containing species were identified: carbon monoxide and dioxide, water, oxygen and nitrogen dioxide. Their presence probably corresponds to desorption, under the effect of thermal treatment, of physisorbed and/ chemisorbed oxygenated compounds. One single gaseous chlorinated species, hydrogen chloride, was detected. The presence HCl can be explained by the fact that nuclear graphite contains between 1 and 15 ppm atomic chlorine and about 20 ppm atomic hydrogen depending on the samples [Chapter 2.I.3).a).ii]. As chlorine has an electronegativity of 3.16 and hydrogen 2.20 on the Pauling scale, then these two atoms can bond covalently to form hydrogen chloride [Handbook of Chemistry and Physics 2008-2009]. In the following paragraph, we will briefly describe the desorption of these gaseous oxygenated and hydrogen chloride species between ambient temperature and 800 °C. For all the nuclear graphites studied, figure 4-18 shows the results we obtained by TDP on the desorption of (a) CO_2, (b) CO, (c) H_2O, (d) O_2, (e) NO_2 and (f) HCl.

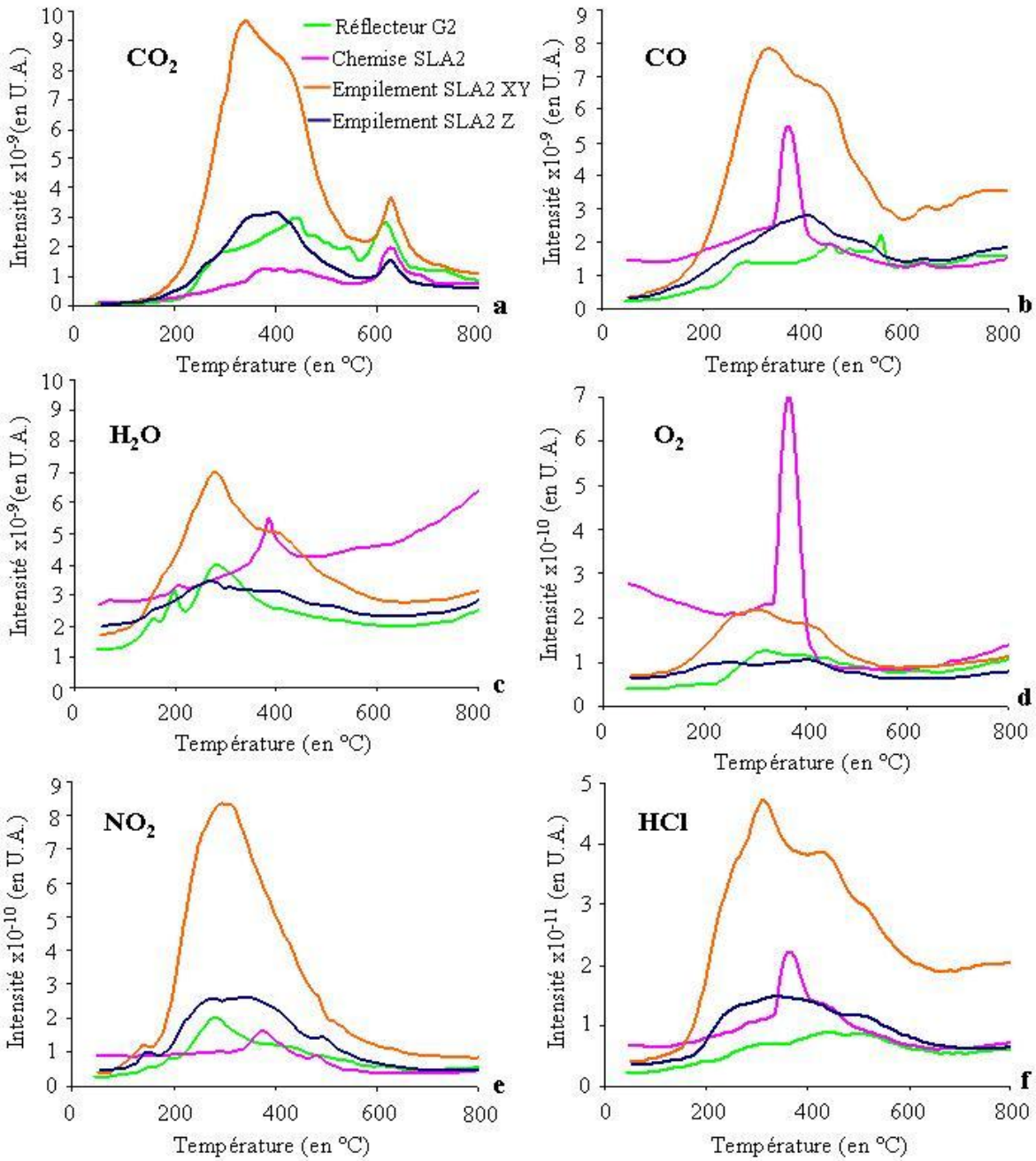

Figure 4-18 : Desorption of (a) CO_2 (b) CO (c) H_2O (d) O_2 (e) NO_2 and (f) HCl between room temperature and 800 °C

As can be seen in figure 4-18a, the desorption of CO_2 occurs in two stages: from 150 to 550 °C, the CO_2 desorption is observed in the form of a large peak. Then, at 625 °C, a narrow peak is observed corresponding to the second stage. This desorption in two steps could correspond to two localizations, of different accessibility, of the CO_2 in the virgin nuclear graphite.

The desorption of CO, as shown on figure 4-18b, occurs in a different manner depending on the nuclear graphite samples studied. In the case of the SLA2 sleeve, desorption took place over quite a limited temperature range, centered around 365 °C. For the G2 reflector and SLA2 moderator samples, the CO desorbs more progressively between 150 and 600 °C. This

difference in desorption temperature is perhaps linked to their difference in porosity. In fact, the graphite of the sleeve is less porous than that of the moderator. However, we have previously highlighted the fact that the porosity of the matrix constitutes a preferential pathway for the release of chlorine [Chapter 4.A.I.2).c)]. The different rates of porosity for the sleeve and moderator graphite could therefore explain the difference observed in the desorption temperatures.

As illustrated in figure 4-18c, H_2O desorbs in a relatively different way according to the type of sample analyzed. In the case of the SLA2 sleeve, H_2O desorbs mainly at about 400 °C. For the G2 reflector, three H_2O desorption peaks, between 100 and 350 °C, can be seen. Finally, for the SLA2 moderator, H_2O desorption is observed as two successive peaks at 300 and 400 °C. It is difficult to explain these different desorption temperatures. Nevertheless, it seems that they are directly linked to the nature of the graphite (see tableau 4-1). In fact, all the nuclear graphites were synthesized using the same process, but from different raw materials (petroleum cokes, coal tar pitch, and purifying agents, etc.) [Chapter 2.I.2)]

The desorption of O_2 for the three types of nuclear graphite studied is presented in figure 4-18d. As for CO in the case of the SLA2 sleeve, the desorption of O_2 took place at about 350 °C, whereas for the G2 reflector and SLA2 moderator, they occurred over a wider range of temperatures, between 150 and 500°C. As stated previously, the difference in porosity between the sleeve graphite and those of the reflector and moderator could explain the different desorption temperatures.

For all the samples studied, the desorption of NO_2, which occurs between 150 and 500 °C, is presented in figure 4-18e.

As shown in figure 4-18f, HCl desorbs between 200 and 600°C, with the peak centered at 350 °C, then a shoulder at about 450 °C. This desorption in two stages seems to be the signature of the existence of two localizations of chlorine, of different accessibility, though it could also be the presence of two chemical forms. Similar results were obtained by par M. Takeda and his team during a study by TDP of different carbons [M. Takeda et al. 2006]. Their conclusion was that this was the result of the presence of two chemical forms of chlorine in the samples.

Finally, for all the oxygenated and chlorinated species detected, gas desorption is influenced by the preferential orientation of the graphite structure (see figure 4-18). In fact, for sample XY, gas desorption begins at lower temperatures than in sample Z, even though samples XY have more accessible pores [Chapter 4.A.I.2).a)]. Once again, these results show that the porosity of the graphite matrix constitutes preferential pathways for the release of oxygenated and chlorinated gas.

B.II.2) Desorption of ethanol

Figure 4-19 shows ethanol desorption (CH_3CH_2OH) under the effect of thermal treatment. The CH_3CH_2OH desorbs in two stages with a peak between 150 and 350 °C, and then a shoulder at around 450 °C. Given that virgin nuclear graphite does not contain ethanol and that this solvent is used when the samples are cut, it is possible that this product is adsorbed at the surface of the matrix. As can be seen on figure 4-19, contrary to other desorbed gaseous species coming from the sample bulk, the desorption of ethanol is not influenced by the

preferential orientation of the nuclear graphite structure. In fact, ethanol begins to be desorbed at the same temperature for the XY and Z SLA2 samples.

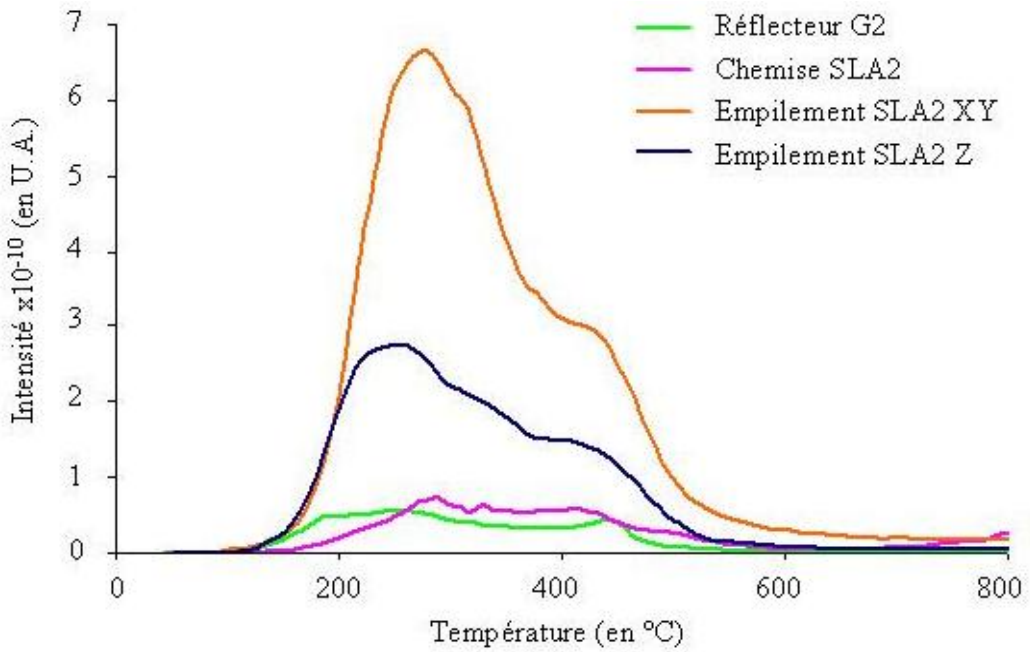

Figure 4-19 : Desorption of CH_3CH_2OH between room temperature and 800 °C

B.II.3) Conclusion

For all the nuclear graphite samples studied by TDP coupled with mass spectrometry, seven gaseous species have been identified. As this analytical technique is not quantitative in our case, it is impossible to realize an inter-sample comparison of the quantities of gas desorbed [Chapter 3.II.2).a)]. Nevertheless, the quantities of gas desorbed from the same sample can be compared. Carbon dioxide and monoxide and water are the species desorbed in the largest quantities, whereas hydrogen chloride is the species desorbed in the smallest quantity. In fact, for a given sample, there is about 150 times fewer chlorinated species desorbed than carbon dioxide and monoxide.

Furthermore, we have shown that desorption of all gaseous species coming from the compounds present in the total volume of the graphite is influenced by the preferential orientation of the matrix structure. Gas desorption, including chlorinated gases, therefore seems to occur via the pores of the graphite. This result is in agreement with those obtained during the study of the thermal behavior of chlorine implanted in nuclear graphite [Chapter 4.A.I.2).c)]. In fact, the porosity of nuclear graphite has been identified as the preferential pathway for the release of implanted chlorine.

Finally, only one detected gaseous species is chlorinated: hydrogen chloride. No desorption of chlorine was observed. Hydrogen chloride desorbs in two stages and seems to imply the existence of two localizations, of different accessibility, of the chlorine or two chemical forms [M.Takeda et al. 2006]. In order to test these hypotheses, XPS and XANES analyses, presented in the next section, were done.

B.III Evolution of the nuclear graphite density and mass during thermal treatment

In order to verify that the TDP experiments do not result in oxidation of the samples, and so loss of matter, we followed the evolution of the density and the mass of nuclear graphite during thermal treatment. To characterize the evolution of the density of nuclear graphite, helium pycnometry measurements were taken before and after TDP [Chapter 3.III.2).b)]. The results obtained for the samples of graphite from the SLA2 sleeve, G2 reflector and SLA2 moderator are presented in table 4-7.

	Densité squelette avant TDP	Densité squelette après TDP
Chemise de SLA2	2,08 ± 0,02	1,98 ± 0,02
Réflecteur de G2	2,11 ± 0,02	1,76 ± 0,02
Empilement de SLA2	2,12 ± 0,02	1,91 ± 0,02

Table 4-7 : Densities of three types of nuclear graphite sample measured by helium pycnometry before and after TDP

For all samples, we observed that the density after TDP is slightly lower than that measured before. This decrease can be explained by desorption of a number of gaseous species [Chapter 4.II] and therefore by a loss of matter, during the TDP experiment. To test this hypothesis, we observed the evolution of the nuclear graphite mass for the SLA2 moderator samples during thermal treatment and in inert atmosphere using thermogravimetric analysis (TGA) [Chapter 3.II.2).b)]. Figure 4-20 shows the thermogravimetric curve obtained for a powdered SLA2 moderator sample.

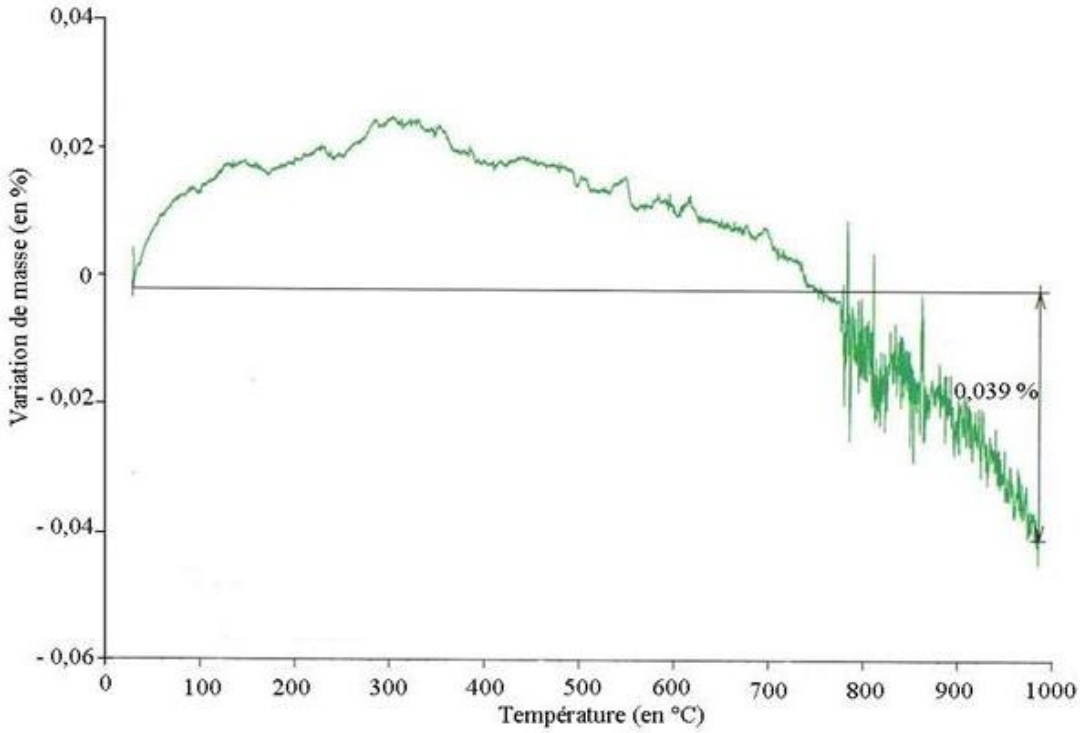

Figure 4-20 : Thermogravimetric curve of a nuclear graphite sample of powdered SLA2 moderator, realized under a nitrogen atmosphere between room temperature and 1000 °C

During thermal treatment and in a nitrogen atmosphere, a mass loss of less than 1 % was measured. This result confirms the slight matter loss obtained previously by helium pycnometry.

B.IV Speciation of carbon and constitutive chlorine by X-ray photoelectron spectroscopy

As indicated in the TDP experiments, desorption of hydrogen chloride occurs in two steps. In order to know if these kinetics are linked to the existence of two localizations of chlorine, of different accessibility or to the presence of two chemical forms, XPS (X-ray photoelectron spectroscopy) analyses were done on nuclear graphite from the SLA2 moderator [Chapter 3.III.3).a)]. Virgin graphite samples, annealed during 4 h at 200, 600 and 1000 °C, were analyzed. The XPS analyses were done on surfaces removed of all pollution. The samples were then cleaved under vacuum just before the analysis. The results obtained are reproducible. These analyses enabled us to study the evolution of the quantity of certain impurities in the nuclear graphite as a function of temperature. Moreover, speciation of the carbon and the constitutive chlorine in the graphite matrix, as well as their evolution with thermal treatment, were characterized. In the rest of this paragraph, for each of the samples the XPS spectral scans and the broadening of the carbon 1s and chlorine 2p peaks are given. For a given sample and for each XPS analysis point, we indicate that the uncertainties in peak area are between 2 and 5 % according to the quantity of element studied, i.e. in the case of carbon 1s and chlorine 2p peak area, the uncertainties are equal to 2 and 4.4 %, respectively.

B.IV.1) Characterization of certain impurities in nuclear graphite

Some of the data available in the bibliography and the analyses by neutron activation of the nuclear graphite indicated the presence of different impurities [Chapter 4.Introduction]. XPS enabled us to realize elemental characterizations. We used this technique in order to complete the results available for virgin nuclear graphite and to obtain data on the evolution of the quantity of impurities with the effect of thermal treatment.

B.IV.1).a) Virgin nuclear graphite

The XPS spectral scans of a virgin graphite sample is given in figure 4-21.

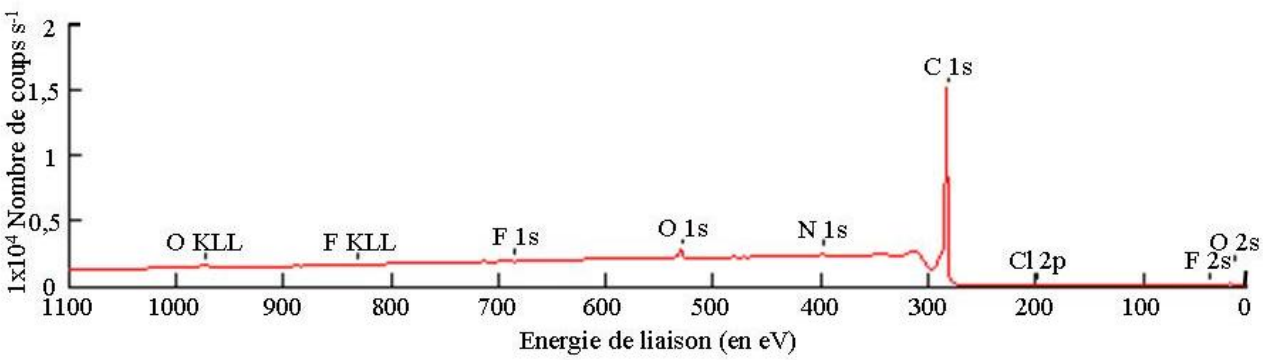

Figure 4-21 : XPS spectral scans of a virgin nuclear graphite sample of the SLA2 moderator

As the sample is mainly composed of carbon, the C 1s peak, with a bond energy of 284.6 ± 0.2 eV, represents 96.5 % atomic of the graphite analyzed. The most abundant impurity is oxygen which reached a rate of 2.5 % atomic. The sample also contains nitrogen (about 1 % atomic) and halogens, i.e. fluorine and chlorine. They are present at rates of 0.1 and less than 0.1 % atomic, respectively.

B.IV.1).b) Effect of thermal treatment

XPS analyses were done on SLA2 moderator samples which had been annealed during 4 h, at 200 and 600°C in inert atmosphere, and 1000 °C under vacuum in order to follow the evolution of the rates of certain impurities. The results are given in figure 4-22.

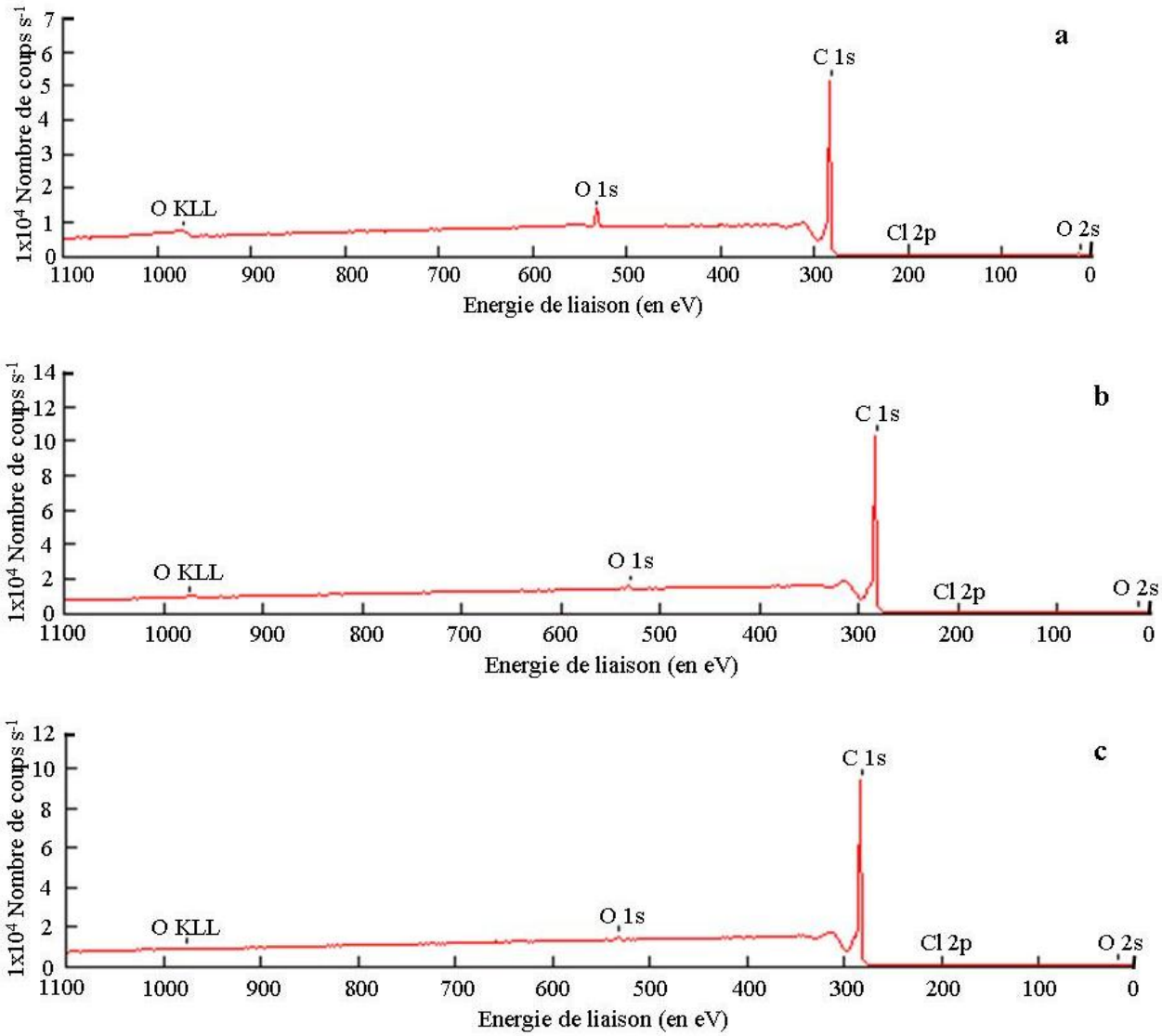

Figure 4-22 : XPS spectral scans of a sample of nuclear graphite from a moderator from SLA2 annealed for 4 h at (a) 200 (b) 600 and (c) 1000 °C

Figure 4-22a shows that from 200 °C the XPS spectral scans of the graphite no longer have any contribution from nitrogen or fluorine. In addition, the rates of chlorine and oxygen have decreased. Figures 4-22 b and c illustrate the fact that at 600 and 1000 °C, the quantity of chlorine continues to decrease as a function of temperature. At 1000 °C, the sample contains about 1 % atomic oxygen and 99 % atomic carbon. The consequence of annealing, whether done in inert atmosphere or under vacuum, results in a reduction of the quantity of the different impurities of the graphite.

B.IV.2) Speciation of carbon in nuclear graphite

To study the carbon speciation of the graphite matrix, we concentrated on the 1s carbon peak (see figures 4-23 and 4-24), where the acquisition necessitated a counting during 50 s.

B.IV.2).a) Virgin nuclear graphite

Figure 4-23 presents the XPS spectrum of the carbon 1s peak obtained for the virgin nuclear graphite of the SLA2 moderator. This spectrum is characteristic on carbonated materials. The principal peak, at 284.6 ± 0.2 eV, corresponds to the contribution of sp^2 hybrid carbons of the aromatic ring. It has an asymmetric shape and the tailing in the direction of increasing energy is linked to the neutralization by conducting electrons, of the holes created during the photoionization. An asymmetric peak is known to be representative of pure graphite [P. M. Th. M. van Attekum and G. K. Wertheim 1979; F. Sette et al. 1990; H. Estrade-Szwarckopf 2004]. Its presence leads to a satellite π-π* peak, situated between 290 and 292 eV [H. Estrade-Szwarckopf 2004]. At around 286.5 eV, the base line to the left of the principal peak is characterized by a higher intensity. This could indicate the presence of carbon atoms covalently bonded to atoms of oxygen [W. H. Lee et al. 2001; H. Estrade-Szwarckopf 2004; G. Speranza et al. 2007].

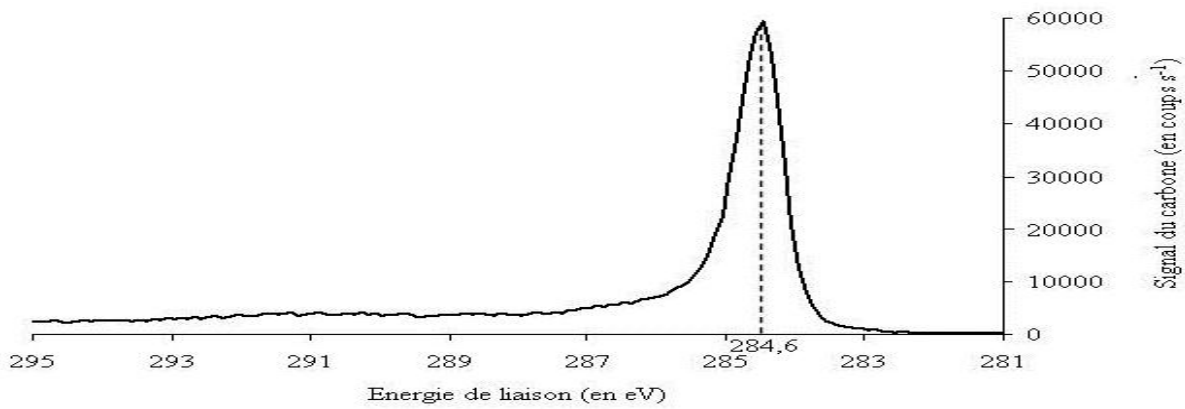

Figure 4-23 : XPS spectrum of the 1s peak of carbon from a sample of virgin nuclear graphite from SLA2 moderator

B.IV.2).b) Effect of thermal treatment

To evaluate the evolution of carbon speciation under thermal treatment, XPS analyses were done on SLA2 moderator graphite samples annealed at 200 and 1000 °C during 4h. The carbon 1s peak obtained for the sample annealed at 1000 °C was subtracted from the one obtained at 200 °C in order to suppress the large contribution from the sp^2 hybridized carbons of the aromatic rings. This procedure allowed us to highlight other contributions (see figure 4-24). In the XPS spectrum obtained, the carbon 1s peak has been divided into its three contributions. The bond energy and corresponding relative area of each of them are presented in table 4-8. The uncertainty of the carbon 1s peak area takes into account the uncertainties from the adjustment procedure and multiple analyses.

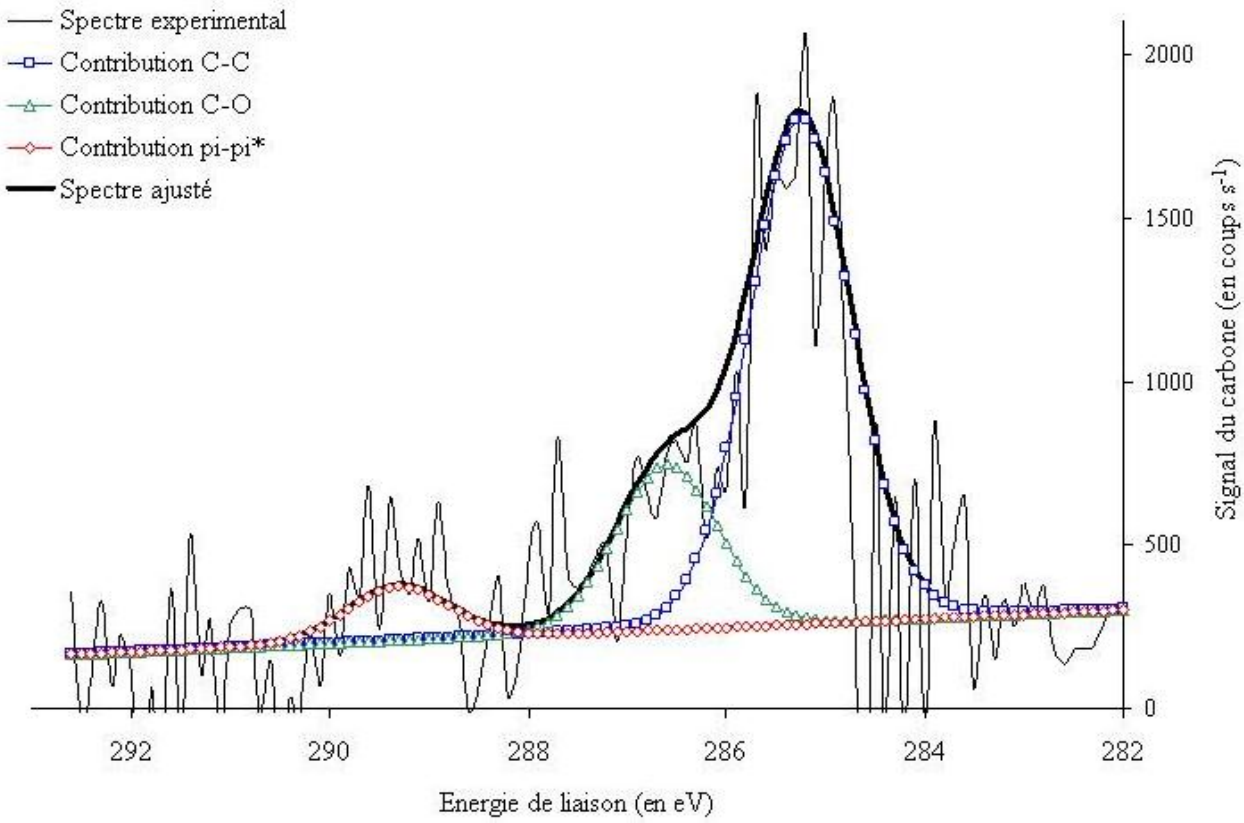

Figure 4-24 : XPS spectrum (experimental and adjusted) resulting from the subtraction of the carbon 1s peak obtained after annealing at 1000 °C from that at 200 °C

Nature de la contribution	Energie de liaison (en eV)	Aire relative (en %)
C-C	285,4 ± 0,2	59 ± 4
C-O	286,5 ± 0,2	21 ± 4
π-π*	289,5 ± 0,2	20 ± 4

Table 4-8 : Nature of the contributions, bond energies and relative peak area for the carbon 1s peak resulting from the subtraction of the XPS spectrum obtained from the sample annealed at 1000 °C from that annealed at 200 °C

The bond energies of the three peaks obtained were attributed to the C-C, C-O and π-π * contributions. The one of C-C corresponds to the covalent bonds between the sp^3 hybridized carbon atoms [G. Speranza et al. 2007]. The C-O contribution is due to the presence of the covalent bonds between the atoms of carbon and oxygen [W. H. Lee et al. 2001; H. Estrade-Szwarckopf 2004; G.Speranza et al. 2007]. The last contribution, π-π*, corresponds to the satellite peak coming from the π-π* transitions [H. Estrade-Szwarckopf 2004]. The relative areas of the different contributions show that the increase in temperature from 200 to 1000 °C leads to a decrease in the relative area of the C-C contribution, which corresponds to the progressive disappearance of the sp^3 hybridized carbon atoms. In the same way, the thermal treatment leads to a breaking of the covalent bonds between the atoms of carbon and oxygen, whose consequence is the release of oxygenated species. This result is coherent with the detection, during the TDP experiments, of five desorbed oxygenated gaseous species of nuclear graphite between ambient temperature and 800 °C [Chapter 4.B.II.1)].

B.IV.3) Speciation of constitutive chlorine in nuclear graphite

To study the constitutive chlorine speciation in nuclear graphite, we concentrated on the 2p chlorine peak (see figures 4-25 and 4-26), where the acquisition requires counting during 35min. As in the case of carbon, the uncertainty of the 2p chlorine peak area takes into account the areas coming from the adjustment procedure and the multiple analyses.

B.IV.3).a) Virgin nuclear graphite

Figure 4-25 presents the XPS spectrum of the chlorine 2p peak obtained for the virgin nuclear graphite of the SLA2 moderator. This peak was divided into four contributions. The nature, bond energy and their relative areas are given in table 4-9.

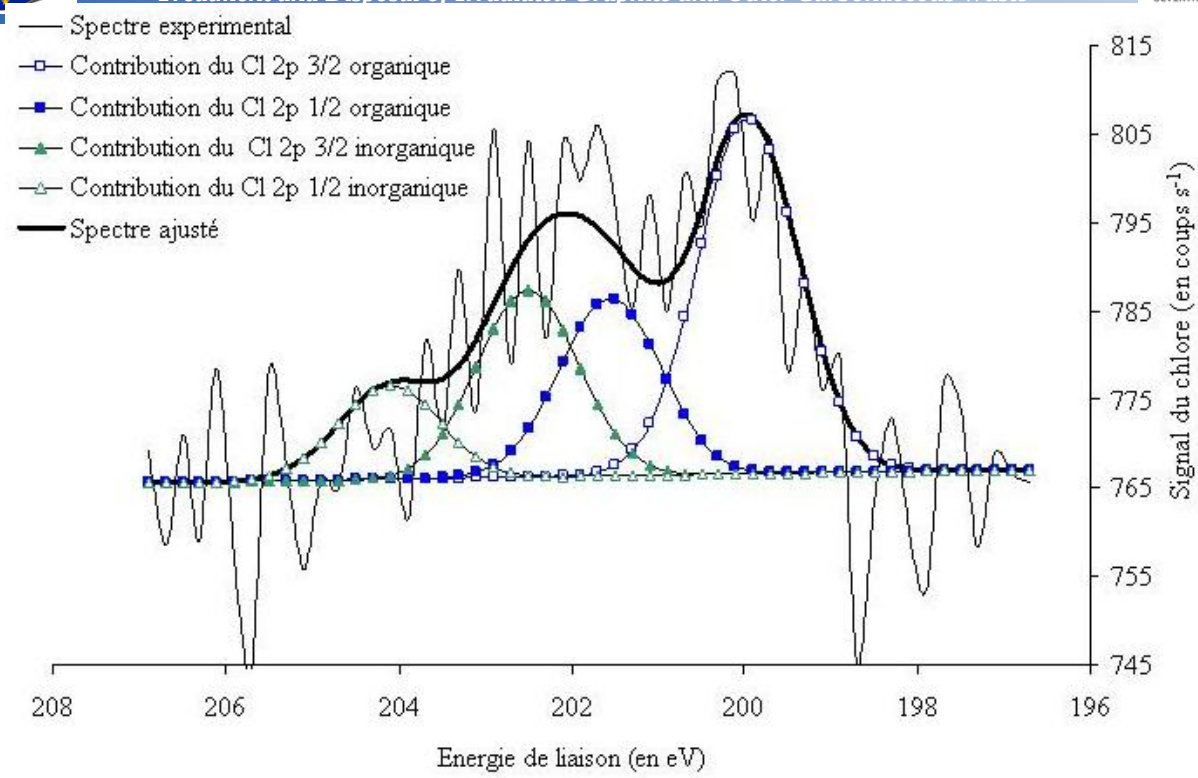

Figure 4-25 : XPS spectrum of the 2p chlorine peak from a sample of virgin nuclear graphite from SLA2 moderator

Nature de la contribution		Energie de liaison (en eV)		Aire relative (en %)	
Chlore organique	$2p_{3/2}$	200,0 ± 0,2	199,9 ± 0,2	70 ± 9	45 ± 9
	$2p_{1/2}$		201,6 ± 0,2		23 ± 9
Chlore inorganique	$2p_{3/2}$	202,5 ± 0,2	202,5 ± 0,2	30 ± 9	21 ± 9
	$2p_{1/2}$		204,1 ± 0,2		11 ± 9

Table 4-9 : Nature of the contributions, bond energies and chlorine 2p relative peak area for a sample of virgin nuclear graphite

After deconvolution of the Cl 2p peak [J. Moulder et al. 1992], we deduced that it is made up of two contributions: one from organic chlorine where the bond energy is 200 ± 0.2 eV and the other from inorganic chlorine with a bond energy of 202.5 ± 0.2 eV [E. Papirer et al. 1995]. Therefore, in the virgin nuclear graphite studied, the constitutive chlorine present is 70 ± 9 % organic and 30 ± 9 % inorganic.

It is important to remember that the organic chlorine corresponds to the chlorine atoms covalently bonded to the sp^2 hybridized carbons in the aromatic rings [E. Papirer et al. 1995; W. H. Lee et al. 2001; A.F.Pérez-Cadenas et al. 2003]. The organic chlorine contribution is itself composed of two peaks: $2p_{3/2}$ $Cl_{organic}$ at 199.95 ± 0.2 eV and $2p_{1/2}$ $Cl_{organic}$ at 201.55 ± 0.2 eV. In our case, the bond energy difference of 1.6 eV between these two peaks is well respected. In addition, the area of the $2p_{3/2}$ $Cl_{organic}$ peak and that of the $2p_{1/2}$ $Cl_{organic}$ are 45 ± 9 and 23 ± 9 %, respectively. These percentages are in agreement with the theoretical data where the $2p_{3/2}$ Cl peak area is double that of the $2p_{1/2}$ Cl peak [A. Barrie et al. 1974].

The inorganic chlorine corresponds to the oxychloride species [E. Papirer et al. 1995]. Its presence can be explained by the fact that the virgin nuclear graphite contains between 1 and 15 ppm atomic chlorine [Chapter 2.I.3).a).ii] and about 2.5 % atomic oxygen [Chapter 4.V.1).a)]. As in the case of organic chlorine, the contribution from inorganic chlorine is composed of two peaks: 2p $_{3/2}$ $Cl_{inorganic}$ and 2p $_{1/2}$ $Cl_{inorganic}$ at 202.5 ± 0.2 and 204.1 ± 0.2 eV, respectively. The 2p $_{3/2}$ $Cl_{inorganic}$ peak area is 21 ± 9 % and that of the 2p $_{1/2}$ $Cl_{inorganic}$ 11 ± 9 %. The bond energy difference and the relation between the two peak areas are, as in the case of organic chlorine, in agreement with the data given in the literature [A. Barrie et al. 1974].

B.IV.3).b) Effect of thermal treatment

The chlorine 2p peak was studied for samples of annealed nuclear graphite in order to follow the evolution of the chlorine speciation under the effect of thermal treatment. Figure 4-26 presents the XPS spectra for the chlorine 2p peak obtained for the samples of nuclear graphite from the SLA2 moderator annealed during 4 h at 200, 600 and 1000 °C. Table 4-10 gathers together the results concerning the relative quantity of chlorine present in the nuclear graphite and the bond energy measured for the Cl 2p peak.

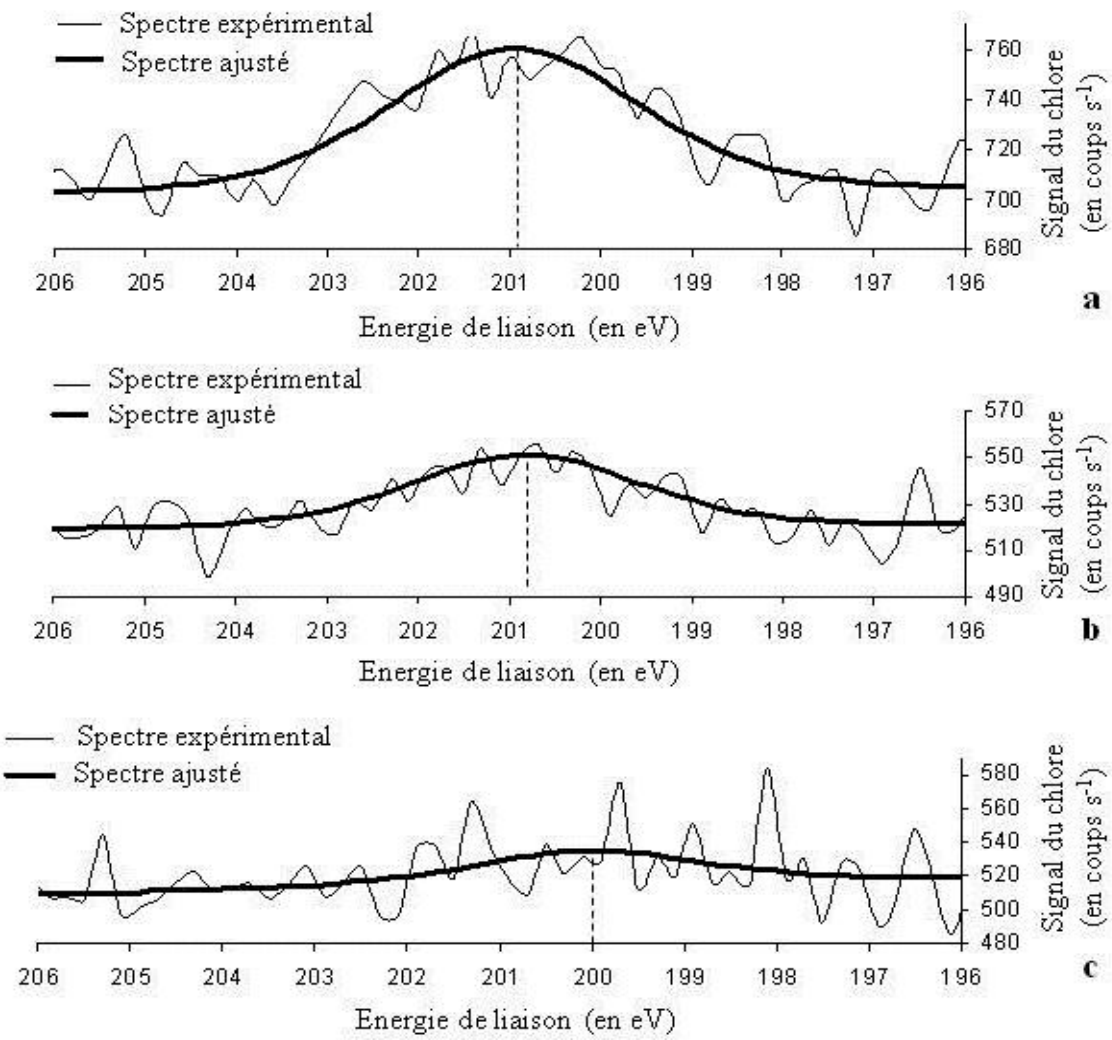

Figure 4-26 : XPS spectra for the chlorine 2p peak for the samples of nuclear graphite from the SLA2 moderator annealed during 4 h at (a) 200 °C, (b) 600 °C, and (c) 1000 °C

Echantillon	Energie de liaison (en eV)	Aire du pic Cl 2p (en nombre de coups s^{-1})
Vierge	200,0 ± 0,2 et 202,5 ± 0,2	115 ± 5
Recuit 200 °C 4h	200,9 ± 0,2	81 ± 12
Recuit 600 °C 4h	200,7 ± 0,2	62 ± 14
Recuit 1000 °C 4h	200,0 ± 0,2	< 30

Table 4-10 : Evolution of the chlorine 2p peak (bond energy and peak area) observed by XPS for the nuclear graphite samples of the SLA2, moderator before and after thermal treatment

As can be seen from the above figure and table, we observe that the Cl 2p peak area decreases with increase in annealing temperature which corresponds to a release of chlorine. The study of the evolution of the bond energies brings information on the evolution of the speciation of chlorine. As we said previously, the virgin samples have two bond energies for the 2p Cl peak: one from the organic chlorine and the other the inorganic chlorine. Between 200 and 1000 °C, the evolution in the bond energy of the 2p Cl peak can be seen by the progressive decrease in the inorganic chlorine contribution. At 1000 °C, only the organic chlorine contribution is observable: the other has totally disappeared. Two chlorinated compounds of different thermal stability were therefore detected in the nuclear graphite. The more labile oxychlorides are released at a lower temperature than the C-Cl groups. This is in agreement with the release of oxygenated species observed previously [Chapter 4.B.II.1) et B.V.2).b)].

B.IV.4) Conclusion

The virgin nuclear graphite from the SLA2 moderator contains 2.5 % atomic oxygen and has certain impurities, one of which is chlorine. The study of the speciation of carbon confirms that the nuclear graphite is mainly composed of sp^2-hybridized carbons from the aromatic rings. Nevertheless, it also contains atoms of sp^3-hybridized carbons. Two speciations of chlorine, having different thermal stabilities, were also observed: the main one is organic (atom of chlorine bonded to an atom of carbon in the aromatic ring) and the other, minor one, is inorganic (oxychlorides).

Our work shows that thermal treatment, between 200 and 1000 °C, leads to the disappearance of the sp^3-hybridized carbon atoms, the release of oxygenated species and inorganic chlorine, consequently revealing that the latter is more thermally labile than the organic chlorine.

B.V Speciation of constitutive chlorine by X-ray absorption spectroscopy

The XPS analyses therefore highlighted the presence of two chemical forms of chlorine, at 70 ± 9 % in the organic form and at 30 ± 9 % for the inorganic form, in the samples of virgin nuclear graphite from the SLA2 moderator. After thermal treatment, chlorine is only detected in the organic form. In order to confirm and complete these results, we characterized the speciation and the degree of oxidation of the constitutive chlorine in the nuclear graphite by X-ray Absorption Near-Edge Structure spectroscopy (XANES). The XANES spectra at the K

threshold of chlorine were recorded for six samples of nuclear graphite. Four of them are virgin samples from the SLA2 moderator, and annealed 4 h at 200 and 600 °C under argon sweeping and at 1000 °C under high vacuum. The two other virgin samples are from the G2 moderator, and annealed for 4 h at 1000 °C under high vacuum. We compared the spectra with those obtained for the different reference compounds in order to identify the speciation and the degree of oxidation of the constitutive chlorine in the nuclear graphite.

B.V.1) Reference compounds

The results concerning the chlorine speciation in the virgin nuclear graphite obtained by XPS, led us to choose two types of reference compound [Chapter 3.III.3).b).ii]. The first contains inorganic chlorine and the second, organic chlorine.

B.V.1).a) Reference compounds containing inorganic chlorine

We determined the K threshold energy of the chlorine for each reference compound containing inorganic chlorine (sodium perchlorate, chlorate, chlorite and chloride) [Chapter 3.III.3).b).ii]. Table 4-11 gives all the threshold energies.

Nom du composé	Formule chimique	Energie du seuil K du chlore
Perchlorate de sodium	$NaClO_4$	2834,0 ± 0,2
Chlorate de sodium	$NaClO_3$	2830,0 ± 0,2
Chlorite de sodium	$NaClO_2$	2826,0 ± 0,2
Chlorure de sodium	NaCl	2826,5 ± 0,2

Table 4-11 : K threshold energies of chlorine for four reference compounds containing inorganic chlorine

The experimental values obtained are in agreement with those published previously by different groups [A. Fillipponi et al. 1993; S. E. Shadle at al. 1994; F. E. Huggins and G. P. Huffman 1995; H. Konishi et al. 2004; Y. Pipon et al. 2007]. The XANES spectra at the K threshold of chlorine, obtained in one scan, for sodium perchlorate, chlorate, chlorite and chloride are shown in figure 4-27.

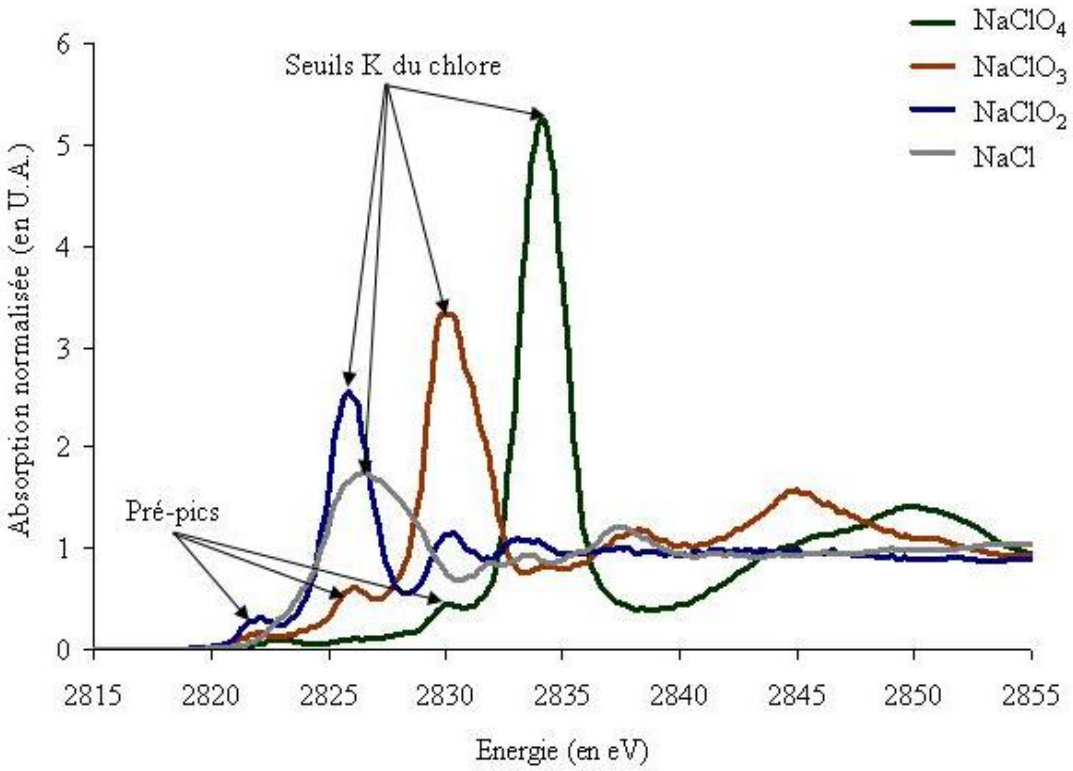

Figure 4-27 : XANES spectra at the K threshold of chlorine for four reference compounds containing inorganic chlorine

The spectrum of sodium chloride is characterized by an absorption threshold at 2826.5 ± 0.2 eV. The spectra of the oxychloride compounds have a similar appearance, with a shoulder of lower intensity, a threshold and the first EXAFS oscillation. The energy of the threshold is between 2826.0 ± 0.2 eV for sodium chlorite (Cl^{+III}) and 2834.0 ± 0.2 eV for sodium perchlorate (Cl^{+VII}). This linear dependence between threshold energy and degree of oxidation of chlorine has already been observed by S. E. Shadle et al. for the KCl, $KClO_3$ and $KClO_4$ series [S. E. Shadle et al. 1994] and by Y. Pipon et al. for the NaCl, $NaClO_2$, $NaClO_3$ and $NaClO_4$ series [Y. Pipon et al. 2007]. Based on this work and by using the threshold energies of the oxychloride compounds determined during our study, we have established the linear relation linking the threshold energies of the chlorine anions and the degree of oxidation of these anions for the series NaClO, $NaClO_2$, $NaClO_3$ and $NaClO_4$. The equation obtained to realize this model is the following:

$$E_0 = 2\,q + 2820$$

Where, E_0 is the threshold energy in eV, and q the degree of oxidation of chlorine. Figure 4-28 presents the evolution of the threshold energy as a function of degree of oxidation of chlorine for the series NaClO, $NaClO_2$, $NaClO_3$ and $NaClO_4$. The threshold energy values for sodium chlorite, chlorate and perchlorate were obtained experimentally, whereas those for sodium hypochlorite were calculated.

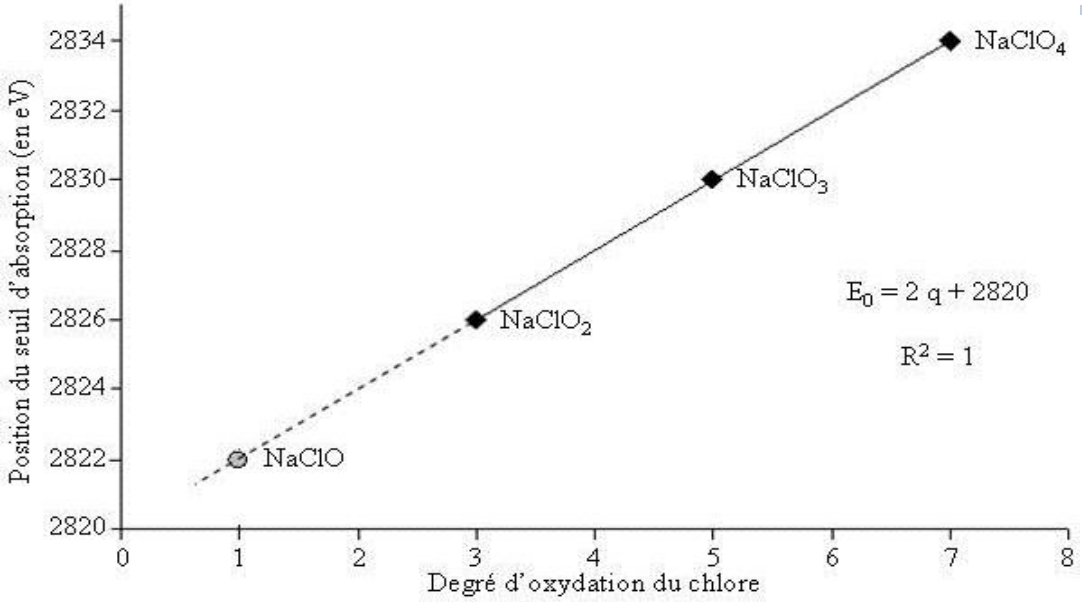

Figure 4-28 : Evolution of the position in energy of the threshold as a function of the degree of oxidation of chlorine

The evolution in the threshold shown in the above figure can be explained by a decrease in the electronic density around the chlorine nucleus [B. Ravel and M. Newville 2005]. In fact, the increase in the number of oxygen atoms leads to an increase in the electronegativity of the ligands.

The XANES spectra of all the oxychloride compounds are characterized by shoulders (see figure 4-27). Two principal reasons can explain their presence: a symmetry effect at the structural site of chlorine or specific energy transition linked to the presence of a ligand [S. E. Shadle et al. 1994], whereas, in the case of oxychlorides, the local structure around the chlorine cannot explain the presence of a shoulder [C. Tarimci et al. 1976; S. C. Abrahams et al. 1977; R. Wartchow et al. 1978]. However, the position in energy of these shoulders seems to indicate that they are not pre-peaks but in fact the presence of another oxychloride of the same cationic series but in a very low quantity. The reference oxychloride compounds are therefore impure.

Under the X-ray beam, an evolution in the chlorine spectra of the oxychloride reference compounds was observed. Figure 4-29 shows the XANES spectra at threshold K for $NaClO_2$, $NaClO_3$ and $NaClO_4$ obtained after two scans at the same point of each pellet.

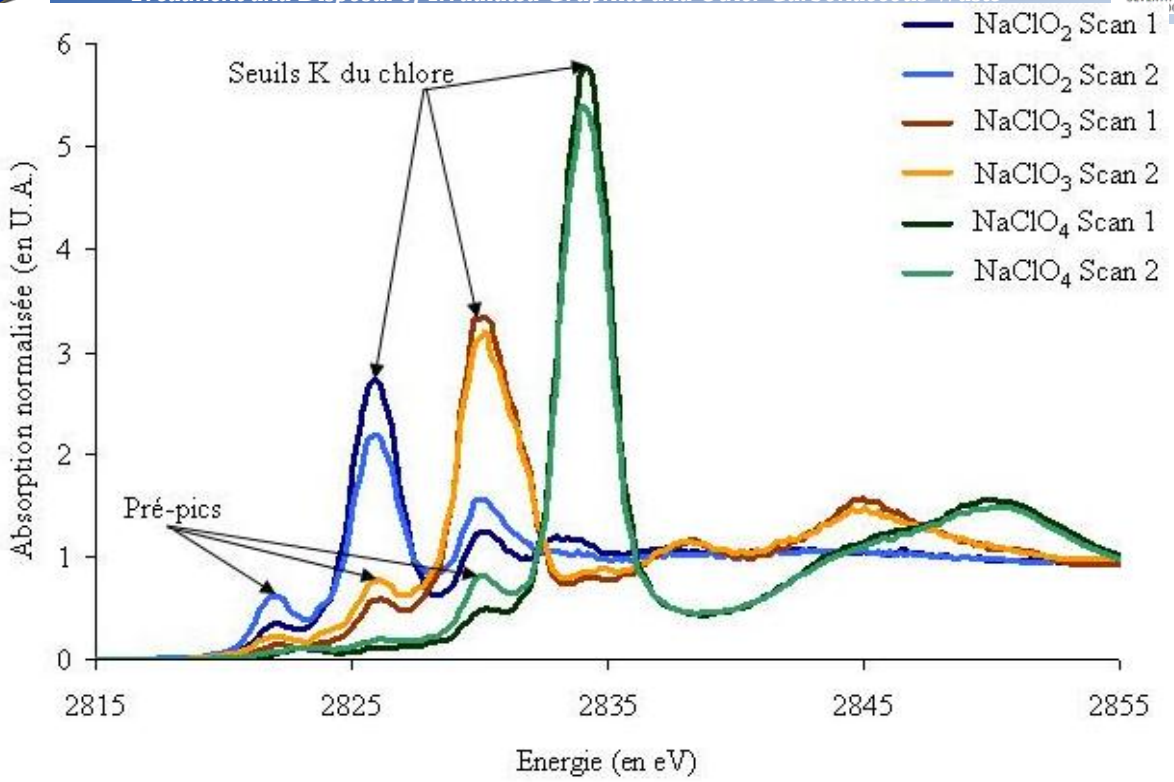

Figure 4-29 : XANES spectra at the K threshold of chlorine for $NaClO_2$, $NaClO_3$ and $NaClO_4$, obtained from two scans realized at the same point of each pellet

By the action of the beam, and for all the oxychlorides analyzed, the intensity of the threshold decreases and that of the shoulder increases. In addition, for $NaClO_2$, the intensity of the first EXAFS oscillation, at 2830.0 ± 0.2 eV, increases. This energy corresponds to that of the threshold for $NaClO_3$. The action of the beam therefore induces a partial oxidation of the $NaClO_2$ into $NaClO_3$. In the same way, the $NaClO_3$ and $NaClO_4$ are partially reduced to $NaClO_2$ and $NaClO_3$, respectively, by the action of the beam.

All the data obtained concerning the stability of the oxychlorides is in agreement with those in the literature [G. Singh et al. 2004]. In fact, the oxychloride compounds are known for their sensitivity to air and/ water and their instability which leads to oxidation reactions, or in the case of sodium perchlorate, exothermic dissociation reactions.

B.V.1).b) Reference compounds containing organic chlorine

Two reference compounds containing organic chlorine, polyvinyl chloride and 2-chloroanthracene, were analyzed [Chapter 3.III.3).b).ii]. Figure 4-30 shows the XANES spectra at threshold K of chlorine obtained in one scan for these two reference compounds. To be clearer, the spectrum of 2-chloroanthracene has been translated along the ordinate axis, and the vertical dotted lines correspond to the K thresholds of chlorine.

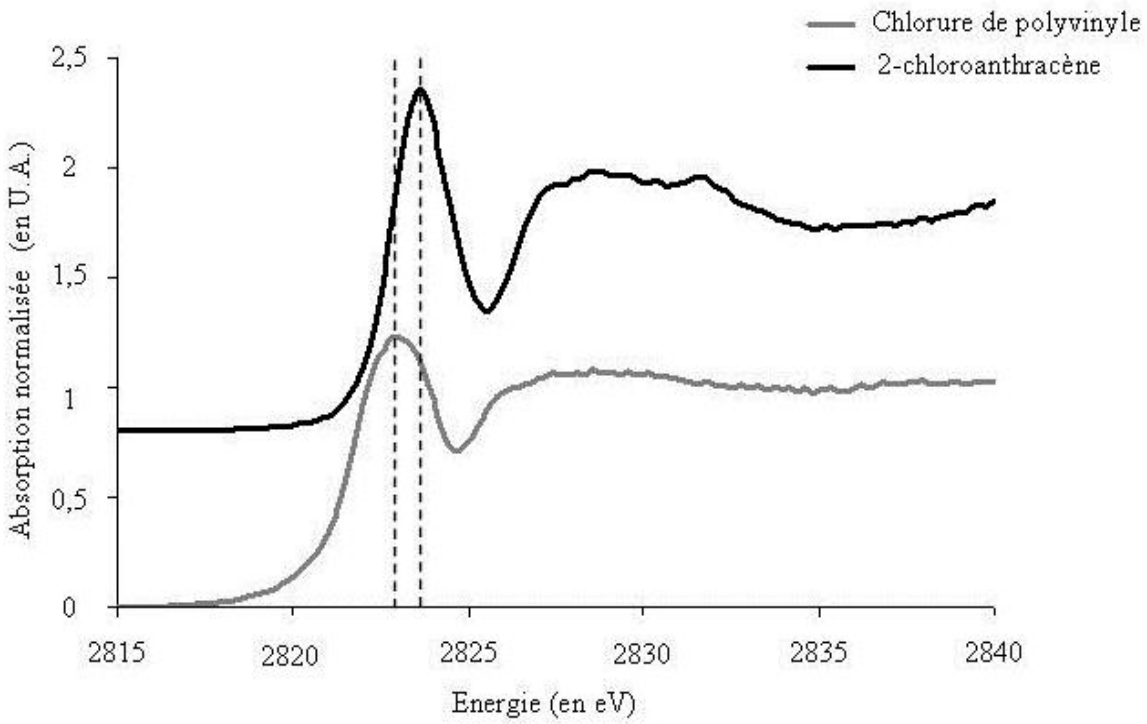

Figure 4-30 : XANES spectra at the K threshold of chlorine for two reference compounds containing organic chlorine

The two spectra in fig.4-30 have a similar shape. They are characterized by an absorption threshold at 2823.0 ± 0.2 and 2823.6 ± 0.2 eV for the polyvinyl chloride and 2-chloroanthracene, respectively, and by the first EXAFS oscillation between 2826 and 2831 eV. The threshold energy and its evolution as a function of the carbon structure to which the chlorine is bonded are in agreement with the data in the literature [S. C. Abrahams et al. 1977; F. E. Huggins and G. P. Huffman 1995; S. Bucher et al. 2002; S. C. B. Myneni 2002; W. Klysubun et al. 2007]. In fact, the threshold energy of an atom of chlorine bonded to an aliphatic chain is less than that of chlorine bonded to an aromatic ring.

In order to test the stability of chlorine, under the action of the beam, for the reference compounds containing organic chlorine, two scans were made at the same point for each of the pellets. Figure 4-31 shows these spectra where the dotted vertical lines correspond to the K thresholds of chlorine.

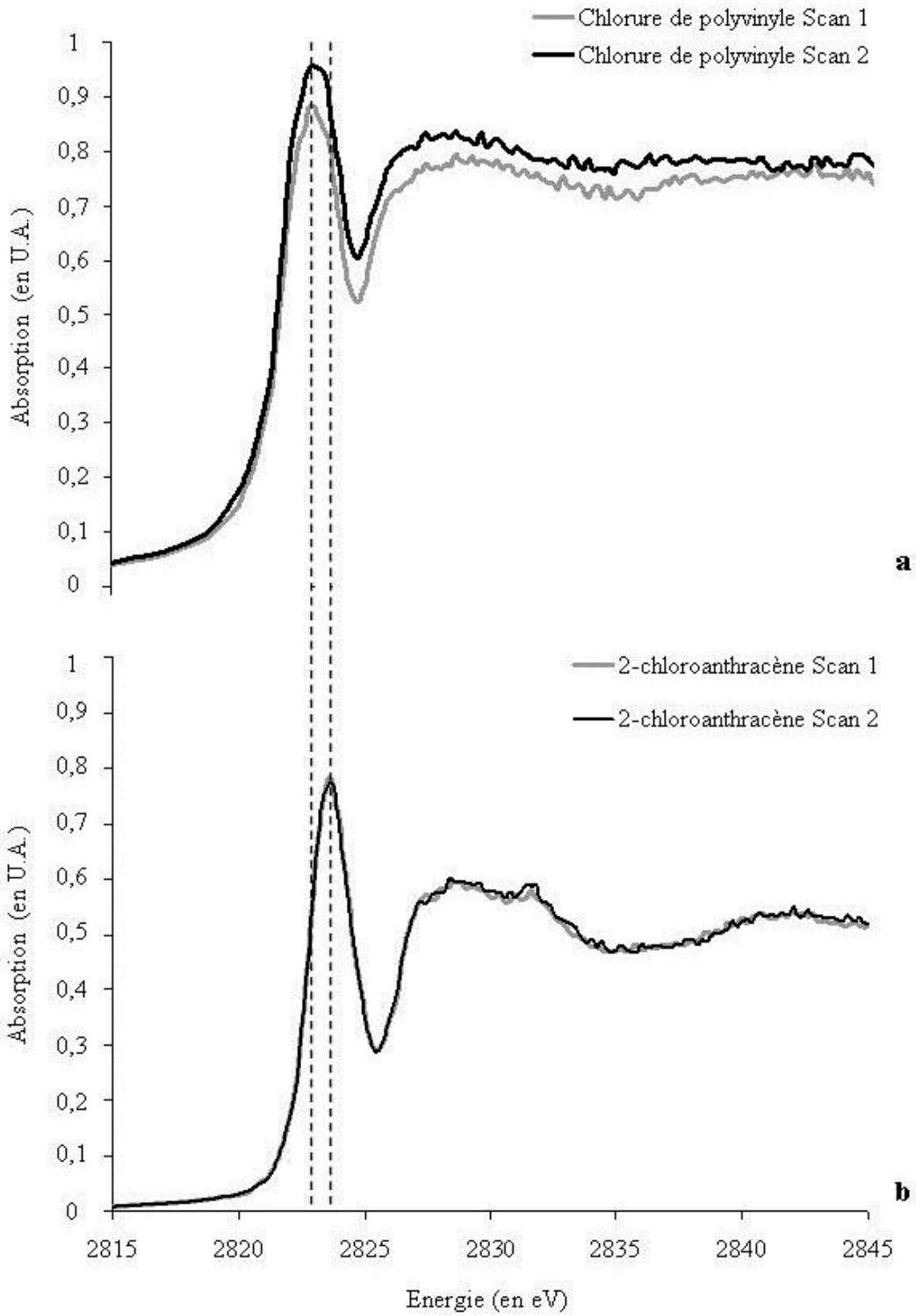

Figure 4-31 : XANES spectra at the K threshold of chlorine (a) of polyvinyl chloride and (b) from 2-chloroanthracene, obtained from two scans realized at the same point on each of the pellets

For the 2-chloroanthracene (see figure 4-31b), the XANES spectra of chlorine, obtained from the first and second scans, are perfectly reproducible. This compound is therefore stable under the beam. However, in the case of polyvinyl chloride (see figure 4-31a), a global variation of the spectrum is observed between the two scans. The action of the beam thus seems to modify the structure of this compound.

As the majority of reference compounds were not stable under the action of the beam, we were then limited in the use of XANES spectra at the K threshold of chlorine obtained in one scan. This precaution allowed us to compare the spectra of the reference compounds with those of the samples in order to characterize the speciation and the valence of the constitutive chlorine of the nuclear graphite without risking any biasing of the results.

B.V.2) Samples of nuclear graphite

Virgin and annealed samples of nuclear graphite of SLA2 and G2 moderators were then analyzed.

B.V.2).a) Stability of chlorine under beam

To study the stability of the constitutive chlorine of the nuclear graphite under the action of the beam, the XANES spectra, obtained from several scans at the same point of our samples were compared. For example, figure 4-32 shows the XANES spectra, obtained after five scans at the same point of our sample of virgin SLA2 moderator.

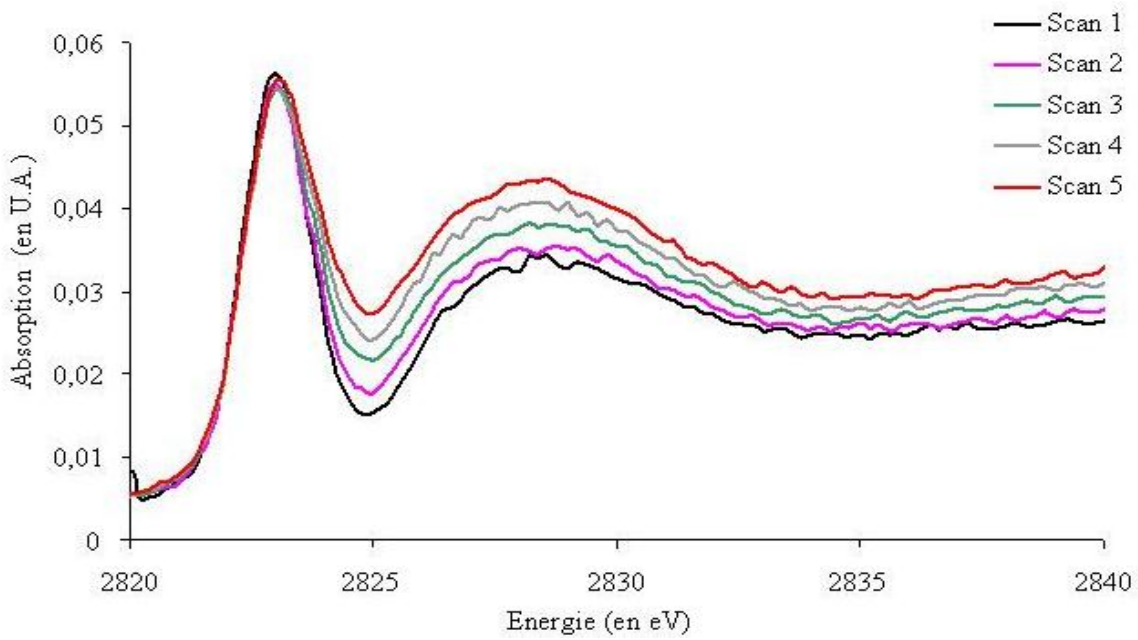

Figure 4-32 : XANES spectra of constitutive chlorine from virgin nuclear graphite from SLA2 moderator, obtained after five scans of the same point on the sample

The appearance, position and intensity of the threshold remain unchanged. Nevertheless, an increase in the intensity of the spectra is observed in the region post-threshold as a function of the time the sample is exposed to the beam. This phenomenon was observed for all the nuclear graphite samples. The experimental conditions used (defocusing of the incident beam and a temperature of –220 °C) to limit the heating up of the samples during the analysis are therefore insufficient in guaranteeing the stability of the chlorine in the beam. Consequently, as for the reference compounds, our study is base on the analysis of the XANES spectra at the threshold K of chlorine, obtained from one scan.

B.V.2).b) Chlorine distribution

To characterize the constitutive chlorine distribution in the nuclear graphite, several scans were recorded at different points on the samples. Figure 4-33 shows the XANES spectra at the threshold K of chlorine, obtained after one scan for two different points of a sample of virgin SLA2 moderator.

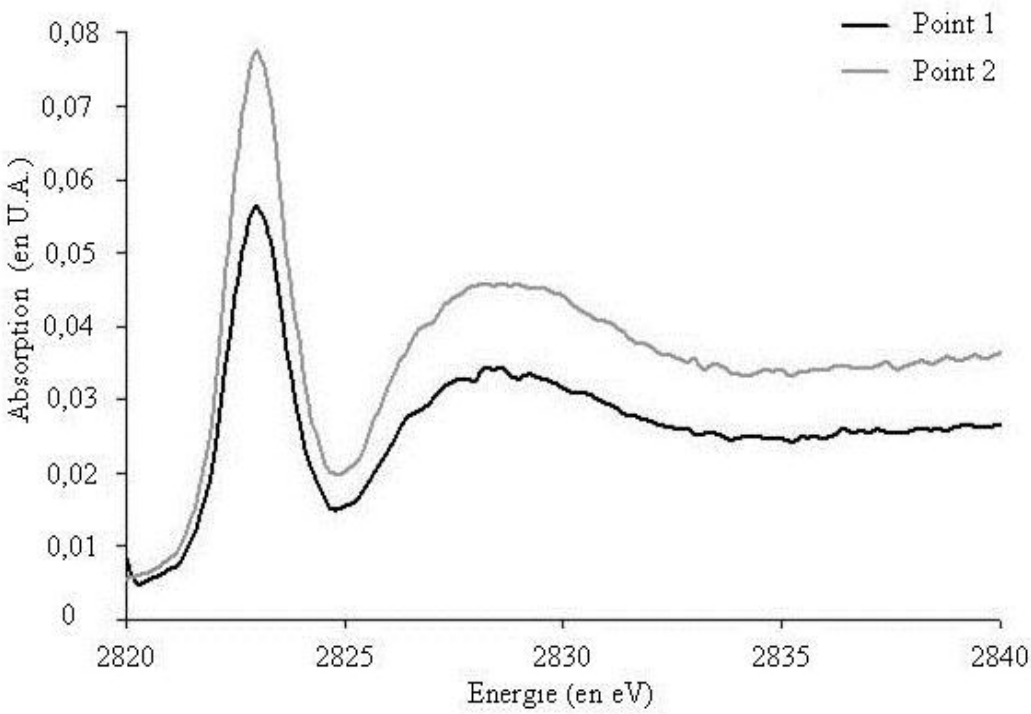

Figure 4-33 : XANES spectra at the K threshold of chlorine of virgin nuclear graphite from SLA2 moderator obtained from a scan at two different points of the sample

The intensity of the spectrum is greater for point 2 than for point 1. As the analytical conditions were the same for both points, the global increase in intensity of the spectrum thus signifies an increase in the quantity of chlorine. The constitutive chlorine distribution in the virgin nuclear graphite is therefore heterogeneous. This result agrees with that obtained by SIMS analysis in image mode [Chapter 4.B.I]. In fact, the mapping of ^{35}Cl in a sample of virgin SLA2 moderator, presented in figure 4-17, showed a heterogeneous distribution of chlorine. Furthermore, the shape of the first EXAFS oscillation is slightly different for the two points. It therefore seems that the environment of the chlorine can be slightly different according to its location in the sample.

B.V.2).c) Virgin nuclear graphite

Figure 4-34 shows the XANES spectra at the threshold K of chlorine for the samples of virgin nuclear graphite of SLA2 and G2 moderator. To be clearer, the spectrum of the G2 moderator has been translated along the ordinate axis and the dotted vertical line corresponds to the threshold K of chlorine.

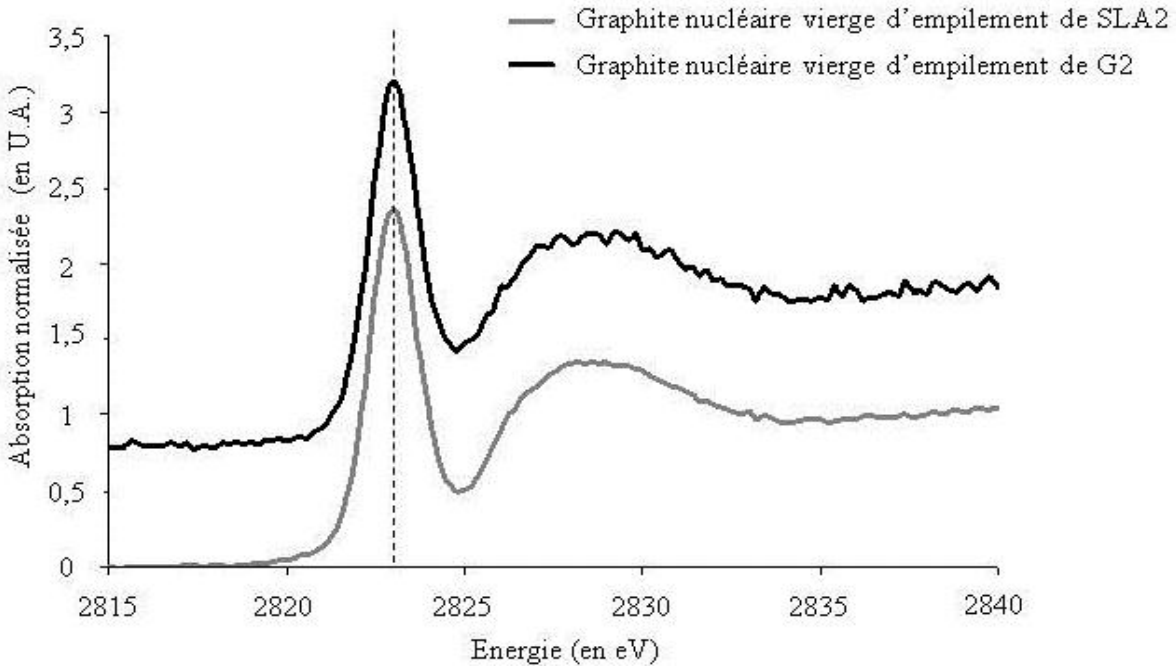

Figure 4-34 : XANES spectra at the K threshold of chlorine for two samples of virgin nuclear graphite from SLA2 and G2 moderators

The two spectra have a similar appearance. They have the same absorption threshold at 2823.0 ± 0.2 eV and the first EXAFS oscillation centered at 2828.6 ± 0.2 eV. We compared these spectra with those of the reference compounds.

- For all the reference compounds containing inorganic chlorine, the position in energy of the absorption threshold is equal or greater to 2826.0 ± 0.2 eV. The samples of virgin nuclear graphite therefore do not contain inorganic chlorine to a degree of oxidation of – I, + III, + V and + VII.
- F. E. Huggins and G. P. Huffman found that in gaseous Cl_2, the position in energy of the absorption threshold of chlorine is equal to 2822.7 ± 0.2 eV [F. E. Huggins and G. P. Huffman 1995]. This value is slightly above that obtained with our samples. It seems therefore that the virgin graphite does not have gaseous chlorine in an oxidation state equal to 0. This result is confirmed by the fact that no intense flash, characteristic of the presence of gas bubbles, was observed during the SIMS analyses [Chapter 4.B.I].
- The elemental composition of graphite (see table 4-2) leads us to think that bonds between the chlorine and metallic impurities, such as iron, nickel or zinc, exist. This type of bond produces a XANES spectrum at the K threshold of chlorine with a pre-peak centered at about 2820 eV [C. Sugiura and T. Suzuki 1981; S. Muramatsu and C.Sugiura 1982; S. E. Shadle et al. 1995; H. Konishi et al. 2004]. Therefore, the absence of pre-peaks on the XANES spectra of our samples proves that chlorine/metal complexes do not exist in virgin nuclear graphite.
- Finally, the spectra of the samples were compared to those of the reference compounds containing organic chlorine. The spectra resemble each other. In addition, the position in energy of the absorption threshold of the samples is equal to that of polyvinyl chloride. However, the energy of the first EXAFS oscillation of the samples is close to that of 2-chloroanthracene.

All of these results therefore enables us to conclude that the constitutive chlorine in virgin nuclear graphite possesses an organic speciation (chlorine is covalently bonded to a carbon chain or aromatic ring) and has a degree of oxidation of – I.

B.V.2).d) Effect of thermal treatment

Figure 4-35 shows the XANES spectra at the K threshold of chlorine for the virgin and annealed samples of SLA2 and G2 moderator. To be clearer, the spectra have been translated along the ordinate axis and the dotted vertical line corresponds to the threshold K of chlorine.

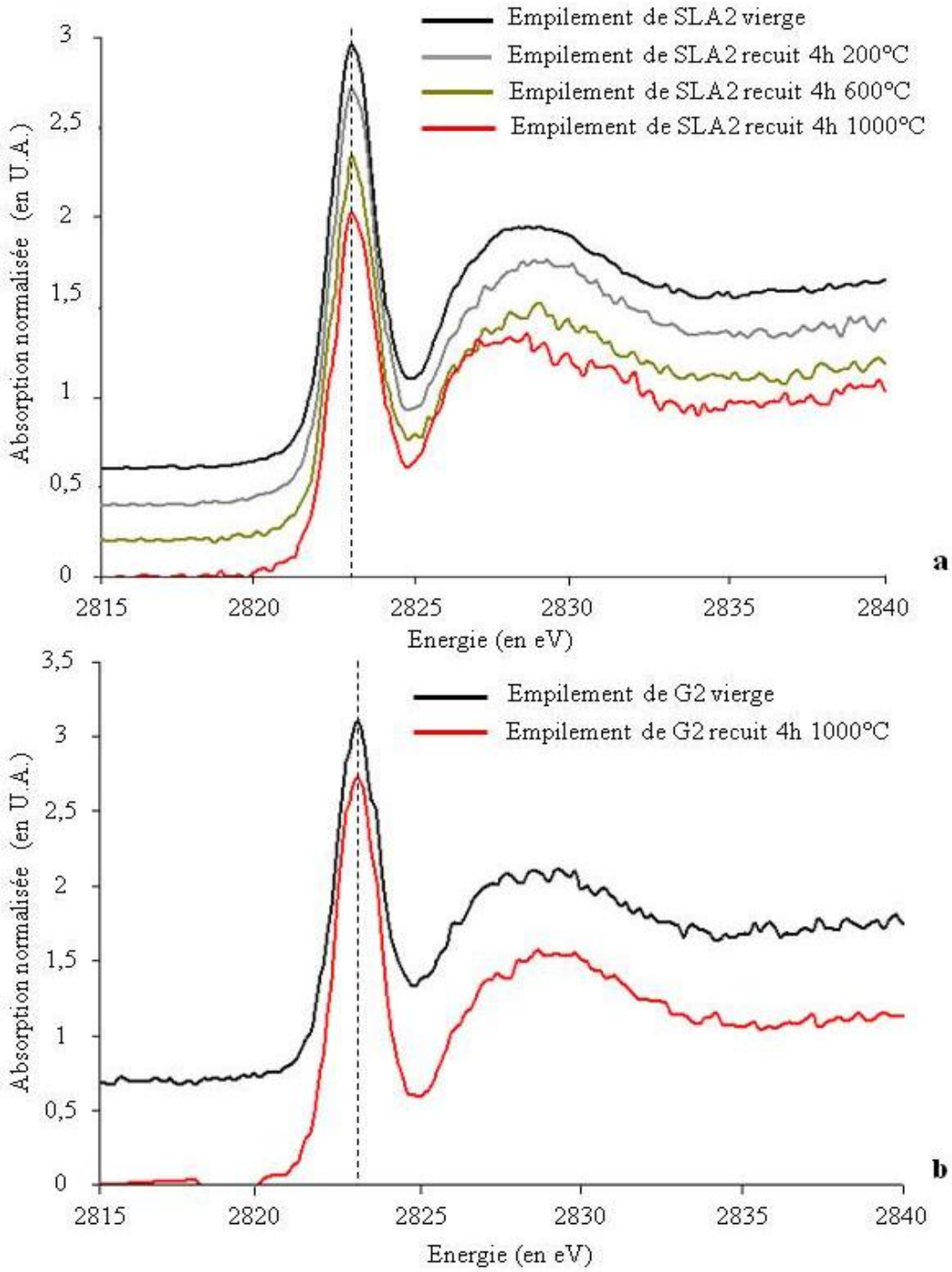

Figure 4-35 : XANES spectra at the K threshold of chlorine from moderators of virgin graphite from (a) SLA2 annealed at 200, 600 and 1000 °C during 4 h and (b) G2 annealed at 1000 °C during 4 h

Due to the effect of thermal treatment, the evolution of the XANES spectra is similar for the two types of moderator. The signal to noise ratio of the spectra decreases as a function of the increase in annealing temperature. This decrease is the signature of a release of chlorine because of the heat treatment. This result is coherent with the data obtained by SIMS and TDP, during our previous studies [Chapter 4.A.I.1) and B.II.3)]. In fact, we have shown that there is a release of chlorine from 200 °C in the form of HCl. However, the thermal treatment does not lead to a change in the position in energy of the threshold of absorption; it remains equal to 2823.0 ± 0.2 eV for both the SLA2 and G2 moderators. Furthermore, no evolution in the shape of the spectra is observed between the virgin and annealed samples. The heat treatment does not appear to induce a change in the chlorine speciation. After thermal treatment, the constitutive chlorine of the nuclear graphite has an organic speciation with a degree of oxidation equal to - I.

B.V.3) Conclusion

The XANES analyses of virgin nuclear graphite from the SLA2 and G2 moderators, have proven the organic speciation and degree of oxidation (– I) of the constitutive chlorine. Nevertheless, from these experiments, it is still difficult to know if the chlorine is bonded covalently to the carbon of the linear chains or the aromatic. To determine which, it is necessary to analyze a larger number of reference compounds containing organic chlorine and in particular, chlorinated intercalation compounds. In fact, in nuclear graphite, the distance between the graphene planes is 3.35 Å, and the negative chlorine with a small anionic radius (1.81 Å), could insert between them. Moreover, even though exploiting the EXAFS part of the spectra would require a long analysis time, it would enable the characterization of the bond distance between the atoms of chlorine and their near neighbors thus completing the information on the speciation and the valence of the chlorine obtained from the XANES spectra.

The thermal treatment leads to a decrease in the quantity of chlorine but changes neither its speciation, nor its degree of oxidation. These results are coherent with those obtained by TDP which show the HCl desorption in which the chlorine has a degree of oxidation of – I [Chapter 4.B.II.3)].

B.VI Conclusion

In this section, we have studied the constitutive chlorine of the nuclear graphite and its thermal behavior. In the virgin nuclear graphite, we have proved the heterogeneous distribution of the constitutive chlorine. In addition, the molecular clusters enriched in chlorine, of a diameter between a nanometer and a micrometer, were observed. Their exact composition is not known. Nevertheless, they do not correspond to the accumulation of oxides as the enriching in chlorine is not correlated with the oxygen enrichment. Moreover, the speciation of the chlorine has been identified by two analytical techniques: XPS and XANES. The results obtained present a similar tendency. The constitutive chlorine of the virgin nuclear

graphite is mainly organic, i.e. that it is bonded covalently to an atom of carbon, and has degree of oxidation equal to – I. A small part (far or less 10 %), corresponds to inorganic chlorine, mainly chlorites, chlorates or perchlorates. These latter forms probably originate from the last purification stages during graphite manufacturing and cover the walls of the pores. There can be two origins of the organic chlorine: on the one hand, the nuclear graphite is synthesized from petroleum coke and coal tar pitch. These carbonaceous raw materials are similar to coal. However, in the literature, this material contains chlorine and the speciation is mainly organic [F. E. Huggins and G. P. Huffman 1995; F. E. Huggins and G. P. Huffman 1996]. Therefore, it is possible that the nuclear graphite be synthesized from carbonaceous materials containing organic chlorine. On the other hand, during the synthesis of nuclear graphite, during the purification step [Chapter 2.I.2).d).iii], chlorine atoms can take the place of certain hydrogen atoms bonded to atoms of carbon in the graphene planes [Chapter 2.II.4)].

We are also interested in the effect of thermal treatment on the behavior of chlorine. From 200 °C, the latter is released, in the form of HCl, via the pores of the nuclear graphite. This desorption takes place in two steps, which could indicate the presence of two locations of chlorine of different accessibility or of two speciations of chlorine. The nuclear graphite being a porous material, it is possible that the chlorine near the open pores is more thermally labile than that in the main volume.

B. Behavior of chlorine during lixiviation

If we take into account the results issued from the experimental leaching tests of ^{36}Cl and chlorine in irradiated graphites obtained by J. Comte and C. Guy from CEA/DEN/LARC (partner 26), their results show that the leaching rate of ^{36}Cl depends both on the position of the sample in the reactor and the temperature of the graphite during reactor operation. The authors show that the release kinetics of the labile fraction of ^{36}Cl in solution can be described by a diffusion process through the graphite porosity. Moreover, they identified two main chemical forms of chlorine in solution: chlorides for the most part on the one hand and chlorites as well as chlorates and perchlorates on the other hand. The chloride/chlorite distribution expressed in moles is about 75 to 90%. It is very interesting to note that our results completely agree with these experimental results. Using different experimental approaches, we have also identified two chemical forms, an organic form and an inorganic one. Moreover, our results show that the inorganic form should be very labile to leaching mainly because of its location on the pore walls (figure 4-36).

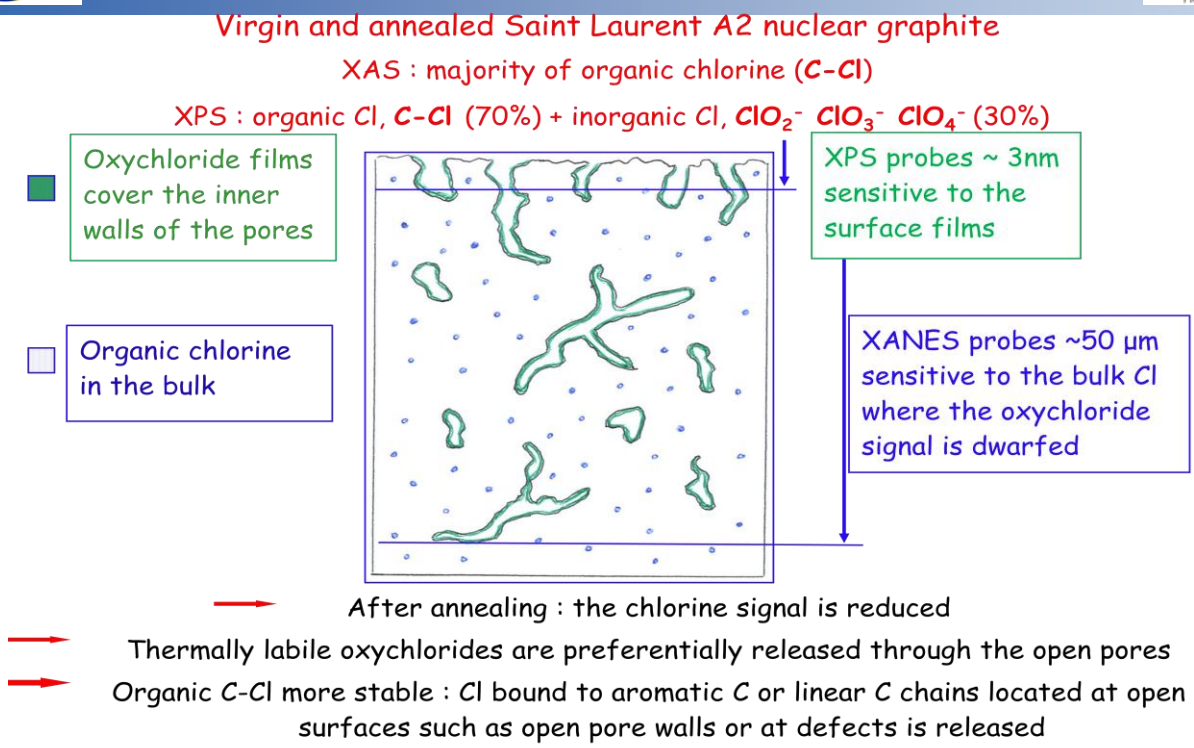

Figure 4-36 : Speciation and location of chlorine in virgin and annealed graphite

J. Comte and C. Guy from CEA/DEN/LARC have also shown that up to 90 % ^{36}Cl can be released in graphite samples issued from “colder”, more irradiated zones of the reactor and therefore less structured zones whereas in “warmer” less irradiated and therefore more structured zones, the release drops to around 10 %.

Our results show that irradiation induces a strong disorder of the graphite matrix and that, during reactor operation, the temperature effect tends to reorder the graphite matrix. The reordering level depends on the temperature but, generally, the graphite does not get its original structure back because this would require very high temperatures (close to graphitization temperatures, i.e. higher than 2000°C). Therefore, depending on the neutron flux distribution in the reactor and the graphite temperature, there will be highly disordered zones with larger pores where chlorine will be more accessible to water and therefore to leaching. On the other hand, in the better structured and less porous zones, chlorine should be less accessible to leaching (figure 4-37).

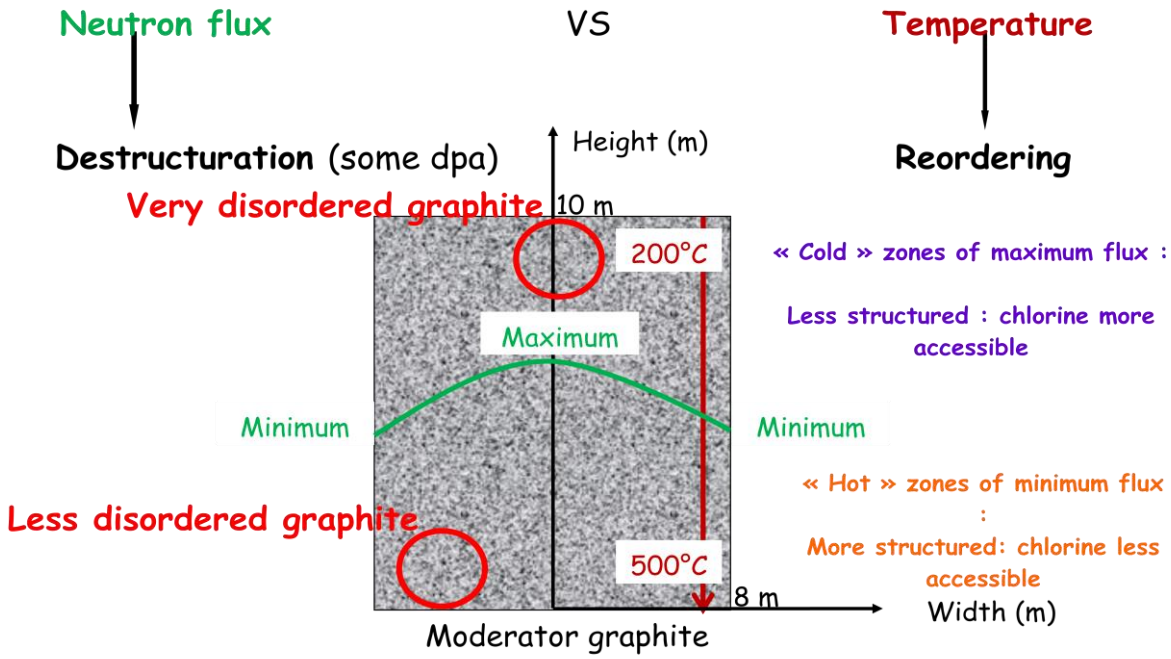

Figure 4-37 : Evolution of the graphite structure during reactor operation

List of figures

FIGURE 4-1 : SCHEMATIC OF THE EXPERIMENTAL PROTOCOL USED FOR STUDYING THE THERMAL BEHAVIOR OF CHLORINE IMPLANTED IN GRAPHITE ----------
FIGURE 4-2 : PROFILES OF THE CONCENTRATION IN ^{37}CL, OBTAINED BY SIMS, FOR THE SAMPLES OF NUCLEAR GRAPHITE FROM THE (A) SLA2 SLEEVE FOR AS-IMPLANTED SAMPLES AND THOSE ANNEALED FOR 2 H AT 200, 400 AND 800 °C, (B) G2 REFLECTOR FOR AS-IMPLANTED SAMPLES AND THOSE ANNEALED FOR 2 H AT 200 AND 800 °C, AND (C) I SLA2 MODERATOR FOR AS-IMPLANTED SAMPLES AND THOSE ANNEALED FOR 4 H AT 600 AND 800 °C----------
FIGURE 4-3 : EVOLUTION OF THE LOGARITHM OF THE RELATION C_T/C_0 AS A FUNCTION OF THE ANNEALING TIMES AT A TEMPERATURE OF 1100 °C FOR A SLEEVE SAMPLE FROM SLA2 ----------
FIGURE 4-4 : ARRHENIUS DIAGRAM OF CHLORINE RELEASE FOR NUCLEAR GRAPHITE SAMPLES FROM (A) THE SLA2 SLEEVE, (B) G2 REFLECTOR, AND (C) SLA2 MODERATOR----------
FIGURE 4-5 : SIMS MAPPING OF ^{37}CL FOR A SAMPLE OF NUCLEAR GRAPHITE FROM THE REFLECTOR OF G2 ANNEALED AT 800 °C DURING 2 H ----------
FIGURE 4-6 : DIAGRAM SHOWING THE SAMPLE GRAINS OF THE SLA2 MODERATOR GRAPHITE WITH XY AND Z ORIENTATIONS, AS WELL AS THE DIRECTION OF ^{37}CL IMPLANTING ----------
FIGURE 4-7 : PROFILES OF AS-IMPLANTED ^{37}CL FOR THE XY AND Z SAMPLES----------
FIGURE 4-8 : LOSS IN ^{37}CL AFTER 4 H OF ANNEALING, AS A FUNCTION OF TEMPERATURE FOR THE XY AND Z SAMPLES ----------
FIGURE 4-9 : ARRHENIUS DIAGRAM OF ^{37}CL RELEASE FOR THE XY AND Z SAMPLES ----------
FIGURE 4-10 : DIAGRAM SHOWING THE GRAPHENE PLANES IN THE HOPG SAMPLES WITH XY' ET Z' ORIENTATIONS, AS WELL AS THE DIRECTION OF THE ^{37}CL IMPLANTING----------
FIGURE 4-11 : MEB IMAGE OF AN HOPG Z' SAMPLE ----------
FIGURE 4-12 : LOSS IN ^{37}CL, AFTER 4 H OF ANNEALING, AS A FUNCTION OF TEMPERATURE FOR THE HOPG XY' SAMPLES ----------
FIGURE 4-13 : RAMAN SPECTRA OF (A) THE SLA2 SLEEVE, (B) G2 REFLECTOR AND (C) SLA2 MODERATOR REALIZED AT THE END OF EACH STEP OF THE EXPERIMENTAL PROTOCOL ----------
FIGURE 4-14 : RAMAN SPECTRA OF HOPG REALIZED AT THE END OF EACH STEP OF THE EXPERIMENTAL PROTOCOL ----------
FIGURE 4-15 : ^{12}C PROFILES OBTAINED BY SIMS FOR (A) TWO SLA2 MODERATOR SAMPLES: ONE POLISHED, THE OTHER POLISHED AND PRE-ANNEALED AT 1000 °C DURING 8 H AND (B) TWO HOPG SAMPLES: ONE VIRGIN, THE OTHER PRE-ANNEALED AT 1000 °C DURING 8 H----------
FIGURE 4-16 : SCHEMATIC REPRESENTATION OF THE EXPERIMENTAL PROTOCOL USED FOR THE STUDY OF THE THERMAL BEHAVIOR OF CONSTITUTIVE CHLORINE IN NUCLEAR GRAPHITE ----------
FIGURE 4-17 : THE SIMS MAPPING OF ^{16}O AND ^{35}CL WITH THE CORRESPONDING OPTICAL IMAGE (INDICATED BY THE BLACK SQUARES) FOR VIRGIN NUCLEAR GRAPHITE FROM THE (A) G2 REFLECTOR AND (B) SLA2 MODERATOR----------
FIGURE 4-18 : DESORPTION OF (A) CO_2 (B) CO (C) H_2O (D) O_2 (E) NO_2 AND (F) HCL BETWEEN ROOM TEMPERATURE AND 800 °C ----------
FIGURE 4-19 : DESORPTION OF CH_3CH_2OH BETWEEN ROOM TEMPERATURE AND 800 °C ----------
FIGURE 4-20 : THERMOGRAVIMETRIC CURVE OF A NUCLEAR GRAPHITE SAMPLE OF POWDERED SLA2 MODERATOR, REALIZED UNDER A NITROGEN ATMOSPHERE BETWEEN ROOM TEMPERATURE AND 1000 °C----------
FIGURE 4-21 : XPS SPECTRAL SCANS OF A VIRGIN NUCLEAR GRAPHITE SAMPLE OF THE SLA2 MODERATOR ---------
FIGURE 4-22 : XPS SPECTRAL SCANS OF A SAMPLE OF NUCLEAR GRAPHITE FROM A MODERATOR FROM SLA2 ANNEALED FOR 4 H AT (A) 200 (B) 600 AND (C) 1000 °C----------
FIGURE 4-23 : XPS SPECTRUM OF THE 1S PEAK OF CARBON FROM A SAMPLE OF VIRGIN NUCLEAR GRAPHITE FROM SLA2 MODERATOR----------
FIGURE 4-24 : XPS SPECTRUM (EXPERIMENTAL AND ADJUSTED) RESULTING FROM THE SUBTRACTION OF THE CARBON 1S PEAK OBTAINED AFTER ANNEALING AT 1000 °C FROM THAT AT 200 °C ----------
FIGURE 4-25 : XPS SPECTRUM OF THE 2P CHLORINE PEAK FROM A SAMPLE OF VIRGIN NUCLEAR GRAPHITE FROM SLA2 MODERATOR----------
FIGURE 4-26 : XPS SPECTRA FOR THE CHLORINE 2P PEAK FOR THE SAMPLES OF NUCLEAR GRAPHITE FROM THE SLA2 MODERATOR ANNEALED DURING 4H AT (A) 200 °C, (B) 600 °C, AND (C) 1000 °C----------
FIGURE 4-27 : XANES SPECTRA AT THE K THRESHOLD OF CHLORINE FOR FOUR REFERENCE COMPOUNDS CONTAINING INORGANIC CHLORINE ----------

FIGURE 4-28 : EVOLUTION OF THE POSITION IN ENERGY OF THE THRESHOLD AS A FUNCTION OF THE DEGREE OF OXIDATION OF CHLORINE----------
FIGURE 4-29 : XANES SPECTRA AT THE K THRESHOLD OF CHLORINE FOR $NaClO_2$, $NaClO_3$ AND $NaClO_4$, OBTAINED FROM TWO SCANS REALIZED AT THE SAME POINT OF EACH PELLET ----------
FIGURE 4-30 : XANES SPECTRA AT THE K THRESHOLD OF CHLORINE FOR TWO REFERENCE COMPOUNDS CONTAINING ORGANIC CHLORINE----------
FIGURE 4-31 : XANES SPECTRA AT THE K THRESHOLD OF CHLORINE (A) OF POLYVINYL CHLORIDE AND (B) FROM 2-CHLOROANTHRACENE, OBTAINED FROM TWO SCANS REALIZED AT THE SAME POINT ON EACH OF THE PELLETS ----------
FIGURE 4-32 : XANES SPECTRA OF CONSTITUTIVE CHLORINE FROM VIRGIN NUCLEAR GRAPHITE FROM SLA2 MODERATOR, OBTAINED AFTER FIVE SCANS OF THE SAME POINT ON THE SAMPLE ----------
FIGURE 4-33 : XANES SPECTRA AT THE K THRESHOLD OF CHLORINE OF VIRGIN NUCLEAR GRAPHITE FROM SLA2 MODERATOR OBTAINED FROM A SCAN AT TWO DIFFERENT POINTS OF THE SAMPLE ----------
FIGURE 4-34 : XANES SPECTRA AT THE K THRESHOLD OF CHLORINE FOR TWO SAMPLES OF VIRGIN NUCLEAR GRAPHITE FROM SLA2 AND G2 MODERATORS ----------
FIGURE 4-35 : XANES SPECTRA AT THE K THRESHOLD OF CHLORINE FROM MODERATORS OF VIRGIN GRAPHITE FROM (A) SLA2 ANNEALED AT 200, 600 AND 1000 °C DURING 4 H AND (B) G2 ANNEALED AT 1000 °C DURING 4 H ----------
FIGURE 4-36 : SPECIATION AND LOCATION OF CHLORINE IN VIRGIN AND ANNEALED GRAPHITE…….
FIGURE 4-37 : EVOLUTION OF THE GRAPHITE STRUCTURE DURING REACTOR OPERATION……..

List of tables

TABLE 4-1 : RAW MATERIALS, PURIFYING AGENTS AND THE CHARACTERISTICS OF THE NUCLEAR GRAPHITE OF THE SLEEVE AND MODERATOR FROM SLA2, AND REFLECTOR AND MODERATOR FROM G2----------
TABLE 4-2 : NATURE AND CONCENTRATION OF THE PRINCIPAL IMPURITIES OF THE GRAPHITE FROM G2 AND SLA2 MODERATORS DETERMINED BY NEUTRON ACTIVATION ----------
TABLE 4-3 : THE FWHM AND PROJECTED RANGE (RP) OF THE ^{37}Cl PROFILES FOR THE SLA2 MODERATOR SAMPLES FOR AS IMPLANTED SAMPLES AND THOSE ANNEALED FOR 4 H BETWEEN 200 AND 1000 °C ----------
TABLE 4-4 : LOSS OF ^{37}Cl AS A FUNCTION OF ANNEALING TEMPERATURE AND FOR A TIME OF 4 H, FOR MODERATOR SAMPLES FROM SLA2----------
TABLE 4-5: QUANTITY OF OXYGEN IN THE SLA2 SLEEVE SAMPLES AFTER BEING SUBMITTED TO DIFFERENT TREATMENT ----------
TABLE 4-6: QUANTITY OF OXYGEN IN THE SLA2 MODERATOR SAMPLES AFTER BEING SUBMITTED TO DIFFERENT TREATMENT ----------
TABLE 4-7 : DENSITIES OF THREE TYPES OF NUCLEAR GRAPHITE SAMPLE MEASURED BY HELIUM PYCNOMETRY BEFORE AND AFTER TDPTABLE 4-8 : NATURE OF THE CONTRIBUTIONS, BOND ENERGIES AND RELATIVE PEAK AREA FOR THE CARBON 1S PEAK RESULTING FROM THE SUBTRACTION OF THE XPS SPECTRUM OBTAINED FROM THE SAMPLE ANNEALED AT 1000 °C FROM THAT ANNEALED AT 200 °C----------
TABLE 4-9 : NATURE OF THE CONTRIBUTIONS, BOND ENERGIES AND CHLORINE 2P RELATIVE PEAK AREA FOR A SAMPLE OF VIRGIN NUCLEAR GRAPHITE ----------
TABLE 4-10 : EVOLUTION OF THE CHLORINE 2P PEAK (BOND ENERGY AND PEAK AREA) OBSERVED BY XPS FOR THE NUCLEAR GRAPHITE SAMPLES OF THE SLA2, MODERATOR BEFORE AND AFTER THERMAL TREATMENT --------
TABLE 4-11 : K THRESHOLD ENERGIES OF CHLORINE FOR FOUR REFERENCE COMPOUNDS CONTAINING INORGANIC CHLORINE----------